



**Department of AERONAUTICS and ASTRONAUTICS
STANFORD UNIVERSITY**

M. UEMURA

NASA CR-50927

POSTBUCKLING BEHAVIOR OF A CIRCULAR CYLINDRICAL SHELL THAT BUCKLES LOCALLY UNDER AXIAL COMPRESSION

PRICES SUBJECT TO CHANGE

Reproduced by
**NATIONAL TECHNICAL
INFORMATION SERVICE**
Springfield, Va. 22151

**MAY
1963**

TECHNICAL REPORT NO. 7
PREPARED FOR THE NATIONAL AERONAUTICS AND SPACE ADMINISTRATION
UNDER GRANT NsG 93-60

**SUDAER
NO. 156**

78

CASE FILE COPY

Department of Aeronautics and Astronautics
Stanford University
Stanford, California

Stanford U., Calif.

POSTBUCKLING BEHAVIOR OF A CIRCULAR CYLINDRICAL SHELL
THAT BUCKLES LOCALLY UNDER AXIAL COMPRESSION

by

Masuji Uemura *May 1963 78 p 13 refs*
Visiting Professor, Stanford University *

(NASA CR - 50927; SUDAER No. 156)
May, 1963

* On leave for 1962 from the Aeronautical Research Institute, Tokyo University, Japan

This work was performed at Stanford University with the sponsorship of the
National Aeronautics and Space Administration under grant NsG-93-60)

(NASA)

ABSTRACT

21045

In view of the experimental evidence that localized diamond-shaped buckling patterns are usually observed in the buckling of cylindrical shells under axial compression, the postbuckling behavior of such shells is analyzed by the use of an asymptotic unperiodic function instead of the periodic buckled pattern previously used by other investigators. After determining the arbitrary coefficients in the deflection pattern so as to satisfy the conditions of continuity along the center line, the postbuckling behavior is determined by the method of solution previously used, that is, from the minimum condition of the total potential energy and total strain energy with respect to several parameters for the case of dead-weight loading and for the case of rigid-testing-machine loading, respectively. The analysis shows that nearly square diamond-shaped and damped (in other words, localized) buckled patterns, as usually observed in experiments, give the minimal values of the energy. However, the minimal value of the buckling stress obtained in this paper is higher than the values obtained for the periodic buckled pattern. This may be due to the imperfect satisfaction of the conditions of continuity along the center line and to the inaccuracy of the assumed buckled pattern. For this reason, improvements in this analysis are currently sought.

ACKNOWLEDGMENT

The author would like to express his gratitude to Professor Nicholas J. Hoff for his many valuable suggestions and stimulating discussions, and to Mr. H. Oniki for his checking the programming for the digital computer in the course of the work reported here.

TABLE OF CONTENTS

1.	INTRODUCTION	1
2.	NOMENCLATURE	4
3.	BASIC RELATIONS	8
4.	EQUILIBRIUM AND COMPATIBILITY EQUATIONS	10
5.	APPROXIMATE DEFLECTED SHAPE	12
6.	STRESS FUNCTION	18
7.	DETERMINATION OF ARBITRARY PARAMETERS AND INTEGRATION CONSTANTS	24
8.	DETERMINATION OF POSTBUCKLING BEHAVIOR	35
9.	NUMERICAL RESULTS	48
10.	DISCUSSION	64
	REFERENCES	72

LIST OF FIGURES

<u>Fig.No.</u>	<u>Page</u>
1. Notation and sign convention	11
2. Assumed deflected shape	11
3. Comparison of two damping functions	16
4(a). Variation of $(\sigma R/Et)_0$ against ω as a function of φ for the specific value $\mu = 1.05$	49
4(b). Variation of $(\epsilon R/t)_0$ against ω as a function of φ for the specific value $\mu = 1.05$	50
4(c). Variation of η_0 against ω as a function of φ for the specific value $\mu = 1.05$	51
5(a). Variation of W_s'' against $(\epsilon R/t)_0$ as a function of φ for the specific value $\mu = 1.05$	52
5(b). Enlargement of Fig.5(a) in the region of small values of $(\epsilon R/t)_0$	53
6. Variation of W_s'' against φ as a function of μ for the specific value $(\epsilon R/t) = 0.48$	54
7. Variation of minimal values of W_s'' with respect to φ against μ for the specific value $(\epsilon R/t) = 0.48$	56
8. Variation of the least minimal values of W_s'' against $(\epsilon R/t)$	57
9. Load-end shortening curve which satisfies the minimal conditions with respect to four parameters	58
10. Variation of φ_m against $\epsilon R/t$	59
11. Variation of μ_m against $\epsilon R/t$	59
12. Variation of η_m against $\epsilon R/t$	60
13. Variation of ω_m against $\epsilon R/t$	60
14. Variation of deflection parameter g against φ as a function of μ	62
15. Variation of deflection parameter h against φ as a function of μ	63
16. Change of axial load-end shortening curves as a function of curvature parameter \sqrt{Rt}/L	66
17. Variation of minimal possible buckling stress $(\sigma R/Et)_{\min}$ against curvature parameter \sqrt{Rt}/L	66
18. Wave patterns along the axial line $y = \lambda y/2$ for three typical values of $(\epsilon R/t)$	68
19. Schematic representation of buckling process for the case of rigid-testing-machine loading	70

1. INTRODUCTION

The elastic stability of thin cylindrical shells has recently become important because of an increased application of thin shells in missile structures.

As is well known, the buckling stress value predicted by the linear theory based on small deflections is much higher than the experimental values. Many attempts have been made to explain this large quantitative disparity for cylindrical shells. First, the nonlinear theory based on finite deformations which was successfully introduced by Karman and Tsien^{1*} more than two decades ago, has contributed much to the understanding of the essential reasons for the large discrepancy between classical theoretical and experimental results. However, in this original paper, due to mathematical difficulties encountered in the nonlinear theory, the analysis was carried out by specifying some parameters in an arbitrary manner; in this respect, the study was not complete from the physical point of view. Thereafter, the "jump" or "snap through" theory has been improved and enlarged by the cumulative efforts of subsequent investigators^{2,3,4,5,6}. For example, more general treatments in which the ratio of wave lengths is determined by the stationary condition were presented by Leggett et al² and Michielsen³, and a more rigorous calculation of the postbuckling behavior of a perfect cylindrical shell was presented by Kempner⁵. The latter was improved by Almroth⁶ who obtained a lower minimum postbuckling load than Kempner⁵ by considering a larger number of free parameters in the displacement function.

However, all these analyses of the postbuckling behavior of an axially compressed cylinder assume a periodic buckled pattern over the whole surface. As can be seen from the experimental results, this mode of deflection has not been observed, but localized diamond-shaped buckling patterns have usually been found^{7,8}. Yoshimura⁴ showed that

* Superscript numbers indicate entries in the References at the end of the report.

this type of local buckling could take place at a lower stress than the general buckling of the whole surface; an inextensional large-deflection pattern was employed in an analysis based on the energy barrier and the Tsien criterion⁹. The difficulty encountered in such a local buckling problem is that the deflected shape is not exactly polyhedral. If the buckles do not cover the entire surface of the cylindrical shell, part of the shell wall must be subjected to membrane and bending stresses, and the deflected shape cannot be maintained without an external load. Hoff¹⁰ analyzed this local buckling problem, with some simplification, by taking into account the plastic deformation along the ridges separating the buckles.

In this paper, the postbuckling behavior of a circular cylindrical shell under axial compression will be analyzed with the aid of an asymptotic unperiodic function under the assumption of local buckling exhibiting only diamond-shaped two-tier buckles. The work described can be considered as a continuation of the work of the previous investigators^{1,2,3,5,6}. Accordingly, the method of solution employed is the same: thus the analysis starts from an approximate function for w , which contains arbitrary parameters, and the stress function is then determined from the compatibility equation. However, in this case, the assumed deflection pattern was made to satisfy the conditions of continuity at $x = 0$ and thus it applies to both the upper and lower parts of the cylinder. Next, the potential energy is calculated by the use of the membrane stresses and the assumed deflection. The values of the arbitrary parameters can then be determined by applying the principle of stationary total potential energy to the system.

In addition to the disagreement of the buckling loads, the test results show large scatter in all cases, exceeding by far the scatter found in tests with bars and plates. Initial imperfections and the elasticity of the testing machines may have a great effect on the results, and much research work¹¹ has been devoted to a clarification of this situation. However, in this paper, such effects will be disregarded. The local buckling of a thin-walled cylindrical shell

with uniform wall thickness without stiffeners, subjected to a compressive load fixed in the axial direction and uniformly distributed along the circumference, will be considered. The limiting cases in which the shell is loaded in either a dead-weight or a rigid testing machine are discussed.

2. NOMENCLATURE

The following coefficients are all functions of ℓ , p and q :

$A_{\ell pq}, B_{\ell pq}$ = quantities defined by Eq.(22)

$C_{\ell pq}, D_{\ell pq}$ = quantities defined by Eq.(47)

$L_{\ell pq}, K_{\ell pq}$ = quantities defined by Eq.(49)

$J_{\ell pq}, O_{\ell pq}$ = quantities defined by Eq.(27)

$M_{\ell pq}, N_{\ell pq}$ = quantities defined by Eq.(32)

$P_{\ell pq}, Q_{\ell pq}$ = quantities defined by Eq.(47)

The following coefficients are all functions of ℓ , p , q and m :

$X_{\ell pq, m}, Y_{\ell pq, m}$ ($m = 1, 2$) = quantities defined by Eq.(20)

$U_{\ell pq, m}, W_{\ell pq, m}$ ($m = 2$) = quantities defined by Eq.(33)

$R_{\ell pq, m}, S_{\ell pq, m}$ ($m = 0, 1, 2, 3$) = quantities defined by Eq.(55)

Z_{ℓ} a coefficient which is a function of ℓ only,
defined by Eq.(20)

C_r, C_s integral constants in the stress function

$\begin{cases} F_{\ell_i \ell_j p_i p_j q}, G_{\ell_i \ell_j p_i p_j q} \\ H_{\ell_i \ell_j p_i p_j q}, I_{\ell_i \ell_j p_i p_j q} \end{cases}$ quantities which are functions of $\ell_i, \ell_j, p_i, p_j, q$
and defined by Eq.(46)

Y_P, Z_P quantities which are functions of
 $\ell_i, \ell_j, p_i, p_j, q, m_i, m_j$ and defined by Eq.(45)

$D = Et^3/12(1-\nu^2)$ bending stiffness

E modulus of elasticity

F Airy stress function

L half length of shell

R mean shell radius

W_1, W_2, W_p	extensional strain energy, bending strain energy, and potential of applied load, respectively
$\begin{cases} W_1', W_2', W_p' = \\ W_1, W_2, W_p / (\pi t^3 LE/R) \end{cases}$	nondimensional quantities
$\begin{cases} W' = \\ (W_1 + W_2 + W_p) / (\pi t^3 LE/R) \end{cases}$	nondimensional total potential energy
$\begin{cases} W' = \\ (W_1 + W_2) / (\pi t^3 LE/R) \end{cases}$	nondimensional strain energy
$a = \pi/\lambda_x, b = \pi/\lambda_y$	
a_i, b_j, C_ℓ	arbitrary coefficients
ℓ, m, p, q, r, s	positive integers
n	number of circumferential waves
t	wall thickness
u, v, w	axial, circumferential, and inward radial displacements, respectively
x, y	axial and circumferential coordinates on median surface of shell, respectively
$\alpha, \gamma, \delta, \xi$	deflection parameters [see Eq.(18)]
β	damping parameter in axial wave form
$\epsilon_x, \epsilon_y, \gamma_{xy}$	axial, circumferential and shear strains on the median surface
$\kappa_x, \kappa_y, \kappa_{xy}$	changes of curvatures and unit twist of the median surface
2Δ	maximum amplitude of deflection
ϵ	unit end shortening
$\mu = \lambda_y/\lambda_x$	ratio of the circumferential and axial wave lengths
$\varphi = \beta/b$	nondimensional damping coefficient

$$\eta = \left(\frac{t}{R} \right) n^2$$

λ_x, λ_y

axial and circumferential half wave lengths,
respectively

ν

Poisson's ratio

σ

applied average axial compressive stress

$\sigma_x, \sigma_y, \tau_{xy}$

axial, circumferential and shear stresses on
the median surface, respectively (positive in tension)

ω

deflection parameter

The following quantities are all functions of μ and φ :

δ, ξ

quantities defined by Eq.(25)

g, k

quantities defined by Eq.(36)

e, f, h

quantities defined by Eq.(42)

I, M, J, V, T

quantities defined by Eq.(38)

$\textcircled{A} \textcircled{B} \textcircled{C}$

quantities defined by Eq.(58)

$\textcircled{E} \textcircled{F} \textcircled{G}$

quantities defined by Eq.(60)

$\textcircled{H} \textcircled{I} \textcircled{J}$

quantities defined by Eq.(57)

$\textcircled{K} \textcircled{L} \textcircled{M} \textcircled{N}$

quantities defined by Eq.(54)

$\textcircled{P} \textcircled{Q} \textcircled{R}$

quantities defined by Eq.(65)

$\textcircled{S} \textcircled{T} \textcircled{U}$

quantities defined by Eq.(68)

$\textcircled{V} \textcircled{W} \textcircled{Z}$

quantities defined by Eq.(61)

$\textcircled{X} \textcircled{Y}$

quantities defined by Eq.(73)

$\textcircled{M1} \textcircled{M2} \textcircled{MS}$

quantities defined by Eq.(48)

$\textcircled{N1} \textcircled{N3}$

quantities defined by Eq.(50)

$\textcircled{LA} \textcircled{MA} \textcircled{NA}$

quantities defined by Eq.(53)

$$\nabla^4 = \left(\frac{\partial^4}{\partial x^4} \right) + 2 \left(\frac{\partial^4}{\partial x^2 \partial y^2} \right) + \left(\frac{\partial^4}{\partial y^4} \right)$$

suffices "x" and "y" denote differentiation with respect to
x and y , respectively

suffices " ℓ " and "u" denote the lower and upper half of the
cylinder, respectively

3. BASIC RELATIONS

The basic relations necessary for solving the local buckling of an axially compressed thin-walled circular cylindrical shell are given in reference [5] and are reviewed here.

In the following investigation it is assumed that the cylindrical shell is long enough so that the boundary effects at the circular edges may be neglected, and short enough so that there is no danger of buckling as a tubular column.

3.1 Median Surface Strains and Changes of Curvature

With terms up to the second order included, the median surface strain components and the changes of curvature are expressed in terms of the displacement components and their derivatives as follows:

$$\left. \begin{aligned} \epsilon_x &= u_x + \frac{1}{2} w_x^2 \\ \epsilon_y &= v_y + \frac{1}{2} w_y^2 - \frac{w}{R} \\ \gamma_{xy} &= u_y + v_x + w_x w_y \end{aligned} \right\} \quad (1)$$

$$\kappa_x = w_{xx}, \quad \kappa_y = w_{yy}, \quad \kappa_{xy} = w_{xy} \quad (2)$$

3.2 Median Surface Stresses

The axial, circumferential and shear stresses on the median surfaces are given by

$$\left. \begin{aligned}
\sigma_x &= \frac{E}{1-\nu^2} (\epsilon_x + \nu \epsilon_y) = \frac{E}{1-\nu^2} \left[u_x + \frac{1}{2} w_x^2 + \nu \left(v_y + \frac{1}{2} w_y^2 - \frac{w}{R} \right) \right] \\
\sigma_y &= \frac{E}{1-\nu^2} (\epsilon_y + \nu \epsilon_x) = \frac{E}{1-\nu^2} \left[v_y + \frac{1}{2} w_y^2 - \frac{w}{R} + \nu \left(u_x + \frac{1}{2} w_x^2 \right) \right] \\
\tau_{xy} &= \frac{E}{2(1+\nu)} (u_y + v_x + w_x w_y)
\end{aligned} \right\} \quad (3)$$

3.3 Total Potential Energy

The total potential energy is given by the sum of the strain energy W_s and the potential energy of the external force W_p .

The strain energy W_s is composed of the following two parts: the extensional strain energy W_1 , where

$$W_1 = \frac{t}{2E} \int_0^L \int_0^{2\pi R} \left[(\sigma_x + \sigma_y)^2 - 2(1+\nu)(\sigma_x \sigma_y - \tau_{xy}^2) \right] dx dy ; \quad (5)$$

and the bending strain energy W_2 , where

$$W_2 = \frac{D}{2} \int_0^L \int_0^{2\pi R} \left[(w_{xx} + w_{yy})^2 - 2(1-\nu)(w_{xx} w_{yy} - w_{xy}^2) \right] dx dy , \quad (5)$$

in which $D = \frac{Et^3}{12(1-\nu^2)}$.

The potential energy of the axial stresses applied to the ends of the shell can be expressed as

$$W_p = -t \int_0^{2\pi R} (\sigma_x)_{x=L} dy \int_0^L u_x dx . \quad (6)$$

4. EQUILIBRIUM AND COMPATIBILITY EQUATIONS

The equilibrium equations and the natural boundary conditions can be derived by the variational process from the stationary principle of the total potential energy.

The equilibrium equations are

$$\begin{aligned}\frac{\partial \sigma_x}{\partial x} + \frac{\partial \tau_{xy}}{\partial y} &= 0 \\ \frac{\partial \tau_{xy}}{\partial x} + \frac{\partial \sigma_y}{\partial y} &= 0\end{aligned}\quad (7)$$

$$\frac{D}{t} \nabla^4 w = \sigma_x w_{xx} + 2\tau_{xy} w_{xy} + \sigma_y w_{yy} + \frac{\sigma_y}{R}$$

in which $\nabla^4 = \frac{\partial^4}{\partial x^4} + 2 \frac{\partial^4}{\partial x^2 \partial y^2} + \frac{\partial^4}{\partial y^4}$.

The equations of equilibrium in the median surface are identically satisfied by the introduction of the Airy stress function $F(x,y)$ which is defined by the following relations

$$\sigma_x = F_{yy}, \quad \tau_{xy} = -F_{xy}, \quad \sigma_y = F_{xx}. \quad (8)$$

Then the equilibrium equation in the normal direction is reduced to

$$\frac{D}{t} \nabla^4 w = F_{yy} w_{xx} - 2F_{xy} w_{xy} + F_{xx} w_{yy} + \frac{1}{R} F_{xx}. \quad (9)$$

By eliminating u and w from the formulae in Eqs.(1) and by using the stress function, the compatibility equation can be obtained as

$$\frac{\nabla^4 F}{E} = w_{xy}^2 - w_{xx} \cdot w_{yy} - \frac{1}{R} w_{xx}. \quad (10)$$

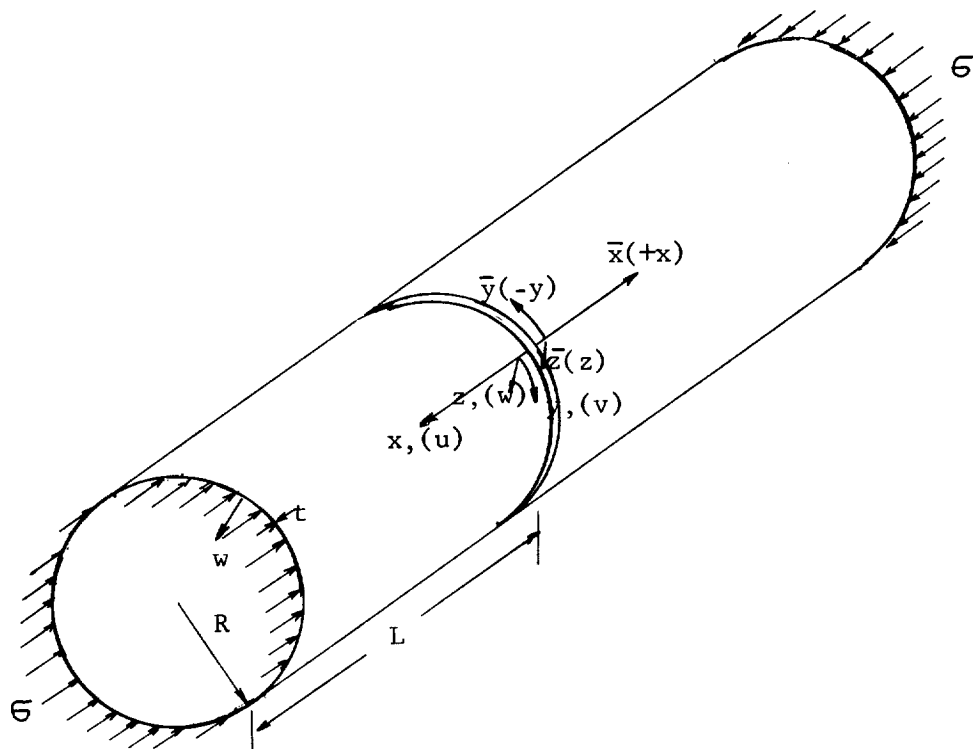


Fig.1 Notation and Sign Convention

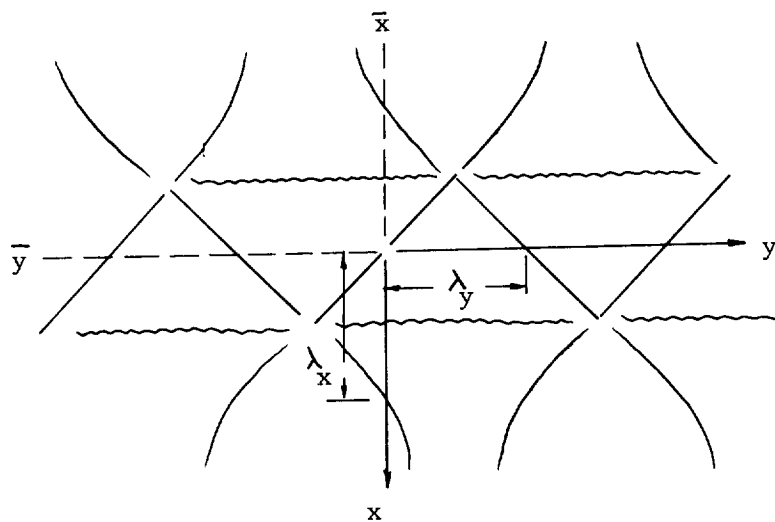


Fig.2 Assumed Deflected Shape

5. APPROXIMATE DEFLECTED SHAPE

It is usually observed in experiments^{4,7,8} that cylindrical shells buckle into the so-called diamond-shaped pattern, exhibiting local inward-buckles of only two tiers as shown in Fig.2. The previously published analyses of the post buckling behavior of an axially compressed cylindrical shell assumed periodic buckling patterns over the whole surface. In this paper, a damped diamond-shaped pattern, as usually observed in tests, will be considered.

The origin of coordinates is taken at the midpoint of a ridge between adjacent diamond-shaped dents as shown in Fig.2, since the deflected pattern is antisymmetric about this point. The x and y coordinates are taken in the axial and circumferential directions, respectively. First, an expression representing an approximate deflected shape for the lower half ($x \geq 0$) of a cylindrical shell will be considered.

A damped diamond-shaped pattern is expressed by the product of two functions as follows:

$$w = w_{\text{damp.}}(x) \cdot w_{\text{dia.}}(x,y) \quad (11)$$

in which $w_{\text{damp.}}$ denotes the damping function and $w_{\text{dia.}}$ denotes the diamond-shaped deflection function.

The $w_{\text{dia.}}$ functions used by several previous investigators are based on the following expression introduced by von Karman and Tsien¹

$$\begin{aligned} w_{\text{dia.}} &= \Delta \left(\sin \frac{\pi}{\lambda_x} x + \sin \frac{\pi y}{\lambda_y} \right)^2 \\ &= \Delta \left(1 - \frac{1}{2} \cos \frac{2\pi x}{\lambda_x} - \frac{1}{2} \cos \frac{2\pi y}{\lambda_y} + 2 \sin \frac{\pi x}{\lambda_x} \sin \frac{\pi y}{\lambda_y} \right) \end{aligned} \quad (12)$$

in which the square is introduced to account for the fact that the shell has a definite preference to buckle inward, and in which λ_x and λ_y are the unknown half wavelengths of the buckles in the axial and circumferential directions.

The expression will be modified in the present paper. The constant coefficients in Eq.(12) will be replaced by arbitrary parameters and more terms will be used in the function of x to make it easier to satisfy the conditions of continuity along the center line ($x = 0$). In addition, the term of $\cos 2by$ in Eq.(12) will be dropped, to take into account the fact that the ridges become very nearly straight after buckling. Accordingly, $w_{dia.}$ is expressed as follows

$$w_{dia.} = \sum_{i=0,2,\dots}^{\text{even}} a_i \cos iax + \sum_{j=1,3,\dots}^{\text{odd}} b_j \sin jax \sin by \quad (13)$$

where $a = \pi/\lambda_x$, $b = \pi/\lambda_y$ and i and j are taken as even and odd integers, respectively, since the deflection pattern is antisymmetrical about the origin of coordinates.

The damping function $w_{damp.}(x)$ is expressed as

$$w_{damp.} = \sum_{\ell=1,2,\dots} C_{\ell} e^{-\ell\beta x} \quad (14)$$

and finally, the approximate deflected shape is represented by

$$w_{\ell} = \sum_{\ell=1,2,\dots} C_{\ell} e^{-\ell\beta x} \left(\sum_{i=0,2,\dots}^{\text{even}} a_i \cos iax + \sum_{j=1,3,\dots}^{\text{odd}} b_j \sin jax \sin by \right) + C_0 \quad (15)$$

by adding a constant term C_0 , which expresses a uniform expansion due to the uniform axial compression.

The conditions of continuity along the y axis ($x = 0$) are as follows. From the continuity of deflection, slope, bending moment and shear force normal to the shell, the following conditions for w can be obtained:

$$w_\ell = w_u \quad (B.1)$$

$$w_{\ell,x} = -w_{u,x} \quad (B.2)$$

$$w_{\ell,xx} = w_{u,xx} \quad (B.3)$$

$$w_{\ell,xxx} = -w_{u,xxx} \quad (B.4)$$

From the continuity of the axial and circumferential displacements, and of the membrane and shearing stresses, the following conditions for u and v can be obtained:

$$u_\ell = -u_u \quad (B.5)$$

$$v_\ell = -v_u \quad (B.6)$$

$$u_{\ell,x} = u_{u,x} \quad (B.7)$$

$$v_{\ell,x} + w_{\ell,x} w_{\ell,y} = v_{u,x} + w_{u,x} w_{u,y} \quad (B.8)$$

The other conditions necessary for the determination of the arbitrary constants are

$$\int_0^{2\pi R} \sigma_x dy = 2\pi R \sigma \quad (B.9)$$

$$\int_0^L \sigma_y dx = 0 ; \text{ zero average circumferential stress} \quad (B.10)$$

v must be a periodic function of y ; the nonperiodic term for y in the expression of v_y should be zero (B.11)

In order to check these conditions along the y -axis by using the same deflected form (Eq.(15)) in both halves, it is enough to replace (y) in the lower half by $(-y)$ in the upper half due to the antisymmetry.

First, in order to satisfy the first four conditions (B.1) to (B.4) for w , it is sufficient to specify w_{damp} only. Thus w becomes

$$w = \omega \frac{t}{\eta} \left[\left(5e^{-\beta x} - 4e^{-2\beta x} + e^{-3\beta x} \right) \left(\sum_{i=0,2,\dots}^{\text{even}} a_i \cos iax \right. \right. \\ \left. \left. + \sum_{j=1,3,\dots}^{\text{odd}} b_j \sin jax \sin by \right) + \gamma \right] \quad (16)$$

More arbitrary coefficients of a_i and b_j should theoretically be retained to satisfy all the other conditions, but this would make the analysis very complicated. Accordingly, for the sake of simplicity, only the important conditions are considered here, and conditions of (B.4) and (B.8) are neglected. This means that the continuity conditions for shearing stresses in the surface plane and normal to the surface are not satisfied. w can be simplified to read

$$w = \omega \frac{t}{\eta} \left[\left(e^{-\beta x} - \frac{1}{2} e^{-2\beta x} \right) \left(\alpha(\delta - \cos 2ax) + 2 \sin ax \sin by \right) + \gamma \right] \quad (17)$$

where δ , α and γ are the arbitrary coefficients to be determined from the other conditions, as will be shown later.

The damping functions in equations (16) and (17) are compared with each other in Fig.3 with a parameter of $\beta' = (\beta \lambda_x)$, from which it can be seen that $(2e^{-\beta x} - e^{-2\beta x})$ is close to $\frac{1}{2}(5e^{-\beta x} - 4e^{-2\beta x} + e^{-3\beta x})$ and is sufficient in accuracy.

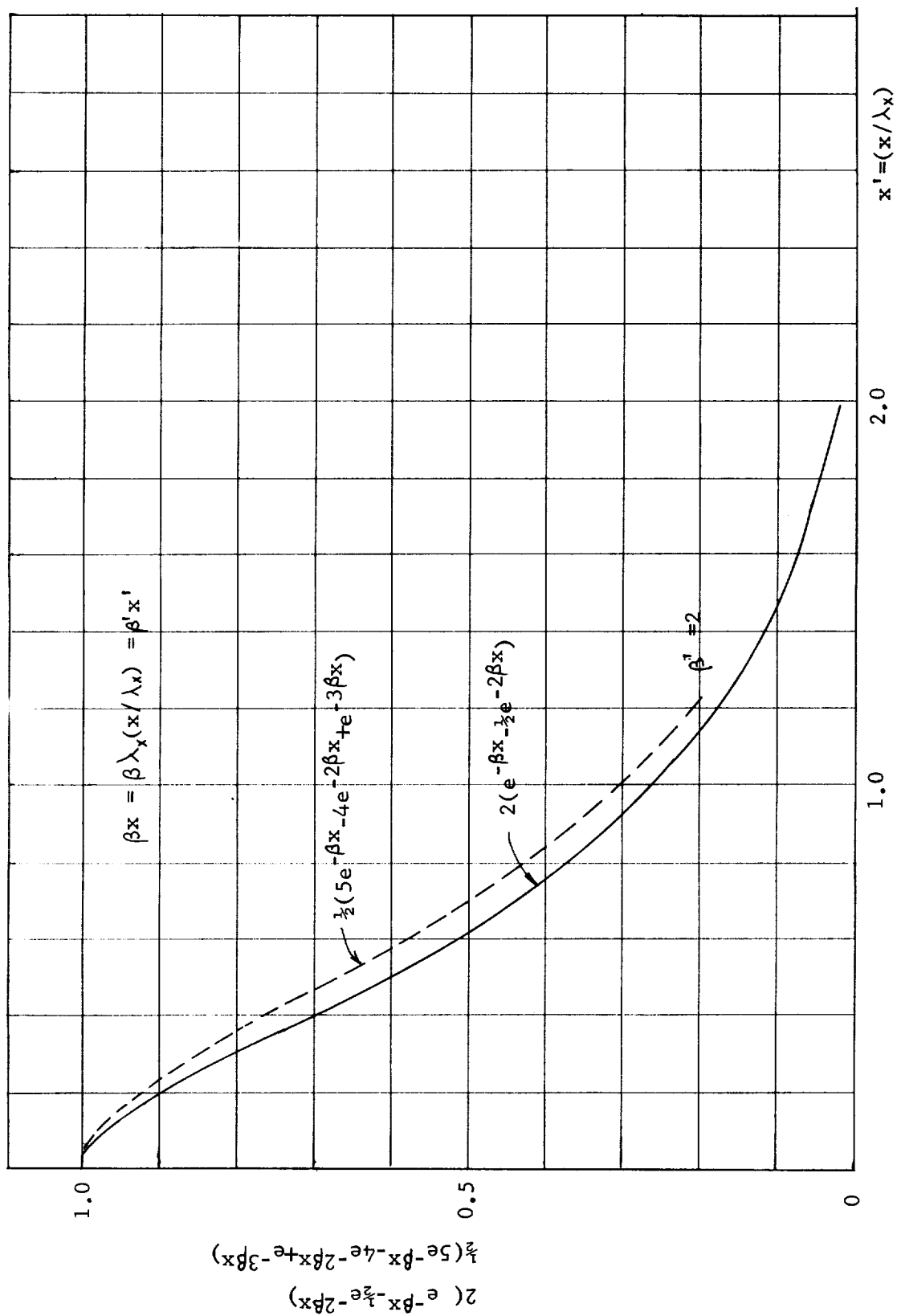


Fig.3 Comparison of two damping functions

Further, in order to prevent δ becoming a function of ω , one more term for ω^2 is added, and then the deflected pattern is finally expressed as

$$w = \omega \frac{t}{\eta} \left[\left(e^{-\beta x} - \frac{1}{2} e^{-2\beta x} \right) \left(\alpha(\delta - \cos 2ax) + 2 \sin ax \sin by \right) + \gamma \right] \\ + \omega^2 \frac{t}{\eta} \xi \left(e^{-\beta x} - \frac{1}{2} e^{-2\beta x} \right) \quad (18)$$

6. STRESS FUNCTION

Equation (10) can be solved to give the stress function F , from which the membrane stresses and hence the displacements u, v can be determined. Introduction of the assumed deflection w of Eq.(18) into the right-hand side of the above equation leads to

$$\begin{aligned}
 \frac{\nabla^4 F}{E} = & -\omega \frac{t^2}{\eta^2} b^4 \sum_{\ell=1,2} \sum_{\substack{p_c=0,2 \\ (p_s=1)}} \sum_{\substack{q_c=0 \\ (q_s=1)}} e^{-\ell\beta x} \left(X_{\ell pq,1} \cos pax + Y_{\ell pq,1} \sin pax \right) \\
 & \times \begin{bmatrix} \alpha \cos q_c by \\ (\sin q_s by) \end{bmatrix} \\
 & + \omega^2 \frac{t^2}{\eta^2} b^4 \sum_{\ell=2,3,4} \sum_{\substack{p_c=0,2 \\ (p_s=1,3)}} \sum_{\substack{q_c=0,2 \\ (q_s=1)}} e^{-\ell\beta x} \left(X_{\ell pq,2} \cos pax + Y_{\ell pq,2} \sin pax \right) \\
 & \times \begin{bmatrix} \cos q_c by \\ (\alpha \sin q_s by) \end{bmatrix} \\
 & - \omega^2 \frac{t^2}{\eta^2} b^4 \xi \varphi^2 (e^{-\beta x} - 2e^{-2\beta x}) \\
 & - \omega^2 \frac{t^2}{\eta^2} b^4 \xi \varphi^2 \sum_{\ell=2,3,4} Z_{\ell} e^{-\ell\beta x} \sin ax \sin by
 \end{aligned} \tag{19}$$

in which

$$X_{100,1} = 8\varphi^2 ,$$

$$X_{200,1} = - 28\varphi^2 ,$$

$$X_{200,2} = 2\varphi^2 ,$$

$$X_{211,2} = - 4\mu\varphi ,$$

$$X_{202,2} = 2\mu^2 ,$$

$$X_{300,2} = - \frac{9}{2} \varphi^2 ,$$

$$X_{302,2} = - \frac{1}{2} (4\mu^2 - \varphi^2) ,$$

$$X_{322,2} = - \frac{\varphi^2}{2} ,$$

$$X_{400,2} = 2\varphi^2 ,$$

$$X_{402,2} = \frac{1}{2} \mu^2 ,$$

$$X_{120,1} = (4\mu^2 - \varphi^2) , \quad Y_{120,1} = - 4\mu\varphi$$

$$Z_2 = - 2 , \quad Z_3 = 5 , \quad Z_4 = - 2$$

$$\left. \begin{array}{ll} X_{111,1} = - 4\mu\varphi , & Y_{111,1} = - 2(\mu^2 - \varphi^2) \\ X_{220,1} = - 2(\mu^2 - \varphi^2) , & Y_{220,1} = 4\mu\varphi \\ X_{211,1} = 4\mu\varphi , & Y_{211,1} = \mu^2 - 4\varphi^2 \\ X_{220,2} = 2(\mu^2 - \varphi^2) , & Y_{220,2} = - 4\mu\varphi \\ X_{231,2} = 4\mu\varphi , & Y_{231,2} = 4\mu^2 - \varphi^2 \\ X_{320,2} = - \frac{1}{2} (4\mu^2 - 9\varphi^2) , & Y_{320,2} = 6\mu\varphi \\ X_{311,2} = 6\mu\varphi , & Y_{311,2} = \frac{1}{2} (8\mu^2 - 5(1+28)\varphi^2) \\ X_{331,2} = - 6\mu\varphi , & Y_{331,2} = - \frac{1}{2} (8\mu^2 - 5\varphi^2) \\ X_{420,2} = \frac{1}{2} (\mu^2 - 4\varphi^2) , & Y_{420,2} = - 2\mu\varphi \\ X_{411,2} = - 2\mu\varphi , & Y_{411,2} = \left\{ \mu^2 - (1+28)\varphi^2 \right\} \\ X_{431,2} = 2\mu\varphi , & Y_{431,2} = (\mu^2 - \varphi^2) \end{array} \right\} \quad (20)$$

The fourth subscripts in the X's and Y's correspond to the numbers of powers of ω .

Through integration of Eq.(19), a general solution of the stress function can be given by

$$\begin{aligned}
 \frac{F}{E} = & - \left(\frac{\sigma}{E} \right) \frac{\gamma^2}{2} + \sum_{r=2,4,\dots} C_r e^{-rbx} \cos rby + \sum_{s=1,2,\dots} C_s e^{-sbx} \sin sby \\
 & - \omega \frac{t^2}{2} \sum_{\ell=1,2} \sum_{\substack{p_c=0,2 \\ (p_s=1)}} \sum_{q_c=0} e^{-\ell\beta x} \left[(A_{\ell pq}^X \ell_{pq,1} - B_{\ell pq}^Y \ell_{pq,1}) \cos pax + (B_{\ell pq}^X \ell_{pq,1} + A_{\ell pq}^Y \ell_{pq,1}) \sin pax \right] \\
 & + \omega^2 \frac{t^2}{2} \sum_{\ell=2,3,4} \sum_{\substack{p_c=0,2 \\ (p_s=1,3)}} \sum_{\substack{q_c=0,2 \\ (q_s=1)}} e^{-\ell\beta x} \left[(A_{\ell pq}^X \ell_{pq,2} - B_{\ell pq}^Y \ell_{pq,2}) \cos pax + (B_{\ell pq}^X \ell_{pq,2} + A_{\ell pq}^Y \ell_{pq,2}) \sin pax \right] \\
 & - \omega^2 \frac{t^2}{2} \frac{\xi}{\varphi} \left(e^{-\beta x} - \frac{1}{8} e^{-2\beta x} \right) \\
 & + \omega^3 \frac{t^2}{2} \frac{\xi \varphi^2}{\eta} \sum_{\ell=2,3,4} Z_{\ell} e^{-\ell\beta x} (B_{\ell 11} \cos ax - A_{\ell 11} \sin ax) \sin by
 \end{aligned} \tag{21}$$

in which

$$A_{\ell pq} = \frac{(p_{\mu}^2 - \ell^2 \varphi^2 + q^2)^2 - 4p^2 \ell^2 \mu^2 \varphi^2}{\left[(p_{\mu}^2 - \ell^2 \varphi^2 + q^2)^2 + 4p^2 \ell^2 \mu^2 \varphi^2 \right]^2}, \quad B_{\ell pq} = \frac{4p \ell \mu \varphi (p_{\mu}^2 - \ell^2 \varphi^2 + q^2)}{\left[(p_{\mu}^2 - \ell^2 \varphi^2 + q^2)^2 + 4p^2 \ell^2 \mu^2 \varphi^2 \right]^2} \quad (22)$$

The membrane stresses are given by

$$\frac{\sigma_x}{E} = \frac{F_{yy}}{E} = -\frac{\sigma}{E} - b^2 \sum_{r=2,4,\dots} C_r e^{-rbx} \cos rby - b^2 \sum_{s=1,3,\dots} C_s e^{-sbx} \sin sby$$

$$\begin{aligned} & + \omega \frac{t^2}{\eta} b^2 \sum_{\ell=1,2} e^{-\ell \beta x} \left\{ (A_{\ell 11} X_{\ell 11,1} - B_{\ell 11} Y_{\ell 11,1}) \cos pax + (B_{\ell 11} X_{\ell 11,1} + A_{\ell 11} Y_{\ell 11,1}) \sin pax \right\} (\sin by) \\ & - \omega \frac{t^2}{\eta} \frac{b^2}{2} \sum_{\ell=2,3,4} \sum_{p_c=0,2} \sum_{q_c=2} e^{-\ell \beta x} \left\{ (A_{\ell pq} X_{\ell pq,2} - B_{\ell pq} Y_{\ell pq,2}) \cos pax + (B_{\ell pq} X_{\ell pq,2} + A_{\ell pq} Y_{\ell pq,2}) \sin pax \right\} \\ & \quad \times \begin{cases} \cos q_c by \\ (\alpha \sin q_s by) \end{cases} \quad (p_s=1,3) \quad (q_s=1) \\ & - \omega \frac{t^2}{\eta} \frac{b^2}{2} \sum_{\ell=2,3,4} Z_{\ell} e^{-\ell \beta x} (B_{\ell 11} \cos ax - A_{\ell 11} \sin ax) \sin by \quad (23a) \end{aligned}$$

$$-\frac{\tau_{xy}}{E} = \frac{F_{xy}}{E} = b^2 \sum_{r=2,4,\dots} C_r e^{-r b x} \sin r b y - b^2 \sum_{s=1,3,\dots} C_s e^{-s b x} \cos s b y$$

$$- \frac{t^2}{\omega} \frac{b^2}{2} \sum_{\ell=1,2} e^{-\ell \beta x} \left\{ \left[(\mu_B \ell_{11} - \ell \varphi_A \ell_{11}) X_{\ell_{11},1} + (\mu_A \ell_{11} + \ell \varphi_B \ell_{11}) Y_{\ell_{11},1} \right] \cos p a x \right. \\ \left. - \left[(\mu_A \ell_{11} + \ell \varphi_B \ell_{11}) X_{\ell_{11},1} - (\mu_B \ell_{11} - \ell \varphi_A \ell_{11}) Y_{\ell_{11},1} \right] \sin p a x \right\} \cos b y$$

$$- \frac{t^2}{\omega} \frac{b^2}{2} \sum_{\ell=2,3,4} \sum_{\substack{p_c=0,2 \\ (p_s=1,3)}} e^{-\ell \beta x} \sum_{q_c=2} e^{-\ell \beta x} q \left\{ \left[(\mu_B \ell_{pq} - \ell \varphi_A \ell_{pq}) X_{\ell_{pq},2} + (\mu_A \ell_{pq} + \ell \varphi_B \ell_{pq}) Y_{\ell_{pq},2} \right] \cos p a x \right. \\ \left. - \left[(\mu_A \ell_{pq} + \ell \varphi_B \ell_{pq}) X_{\ell_{pq},2} - (\mu_B \ell_{pq} - \ell \varphi_A \ell_{pq}) Y_{\ell_{pq},2} \right] \sin p a x \right\} \\ \times \begin{matrix} \sin q_c b y \\ (-\alpha \cos q_s b y) \end{matrix}$$

$$- \frac{t^3}{\omega} \frac{b^2}{2} \sum_{\ell=2,3,4} \sum_{\ell} e^{-\ell \beta x} \left[(\mu_A \ell_{11} + \ell \varphi_B \ell_{11}) \cos a x + (\mu_B \ell_{11} - \ell \varphi_A \ell_{11}) \sin a x \right] \cos b y$$

(23b)

$$\frac{\sigma_y}{E} = \frac{F_{xx}}{E} = b^2 \sum_{r=2,4,\dots} C_r e^{2-rbx} \cos rby + b^2 \sum_{s=1,3,\dots} C_s e^{2-sbx} \sin sby$$

$$+ \omega \frac{t^2}{2} b^2 \sum_{\ell=1,2} \sum_{\substack{p_c=0,2 \\ (p_s=1)}} \sum_{q_c=0} e^{-\ell\beta x} \left\{ \left[\left((p_\mu^2 - \ell^2 \varphi^2)^A \right)_{\ell pq} + 2p\ell\mu\varphi B \right] X_{\ell pq,1} - \left[(p_\mu^2 - \ell^2 \varphi^2)^B \right]_{\ell pq} - 2p\ell\mu\varphi A \right] Y_{\ell pq,1} \cos pax \right. \\ \left. + \left[\left((p_\mu^2 - \ell^2 \varphi^2)^B \right)_{\ell pq} - 2p\ell\mu\varphi A \right] X_{\ell pq,1} + \left[(p_\mu^2 - \ell^2 \varphi^2)^A \right]_{\ell pq} + 2p\ell\mu\varphi B \right] Y_{\ell pq,1} \sin pax \right\} \\ \times \begin{cases} \alpha \cos q_c by \\ (\sin q_s by) \end{cases}$$

$$- \frac{2}{\omega} \frac{t^2}{2} b^2 \sum_{\ell=2,3,4} \sum_{\substack{p_c=0,2 \\ (p_s=1,3)}} \sum_{q_c=0,2} e^{-\ell\beta x} \left\{ \begin{matrix} X_{\ell pq,1} \rightarrow X_{\ell pq,2} & , & Y_{\ell pq,1} \rightarrow Y_{\ell pq,2} \end{matrix} \right\} \begin{matrix} \cos q_c by \\ (\alpha \sin q_s by) \end{matrix}$$

$$- \frac{2}{\omega} \frac{t^2}{2} \xi b^2 (e^{-\beta x} - \frac{1}{2} e^{-2\beta x})$$

$$- \frac{3}{\omega} \frac{t^2}{2} \xi b^2 \varphi^2 \sum_{\ell=2,3,4} Z_\ell e^{-\ell\beta x} \left[\left((p_\mu^2 - \ell^2 \varphi^2)^B \right)_{\ell 11} - 2\ell\mu\varphi A \right] \cos ax - \left[\left((p_\mu^2 - \ell^2 \varphi^2)^A \right)_{\ell 11} + 2\ell\mu\varphi B \right] \sin ax \sin by \quad (23c)$$

The expression for σ_x satisfies the condition of Eq.(B.9) since the integral of the periodic term for y over the circumference reduces to zero. The expression for τ_{xy} satisfies the condition of zero average shear stress.

*The following abbreviation is used throughout the text: the symbol (1) \rightarrow (2) means that the quantity (2) should replace the quantity (1) in the immediately preceding expression to obtain the current one.

7. DETERMINATION OF ARBITRARY PARAMETERS AND INTEGRATION CONSTANTS

The arbitrary parameters in the approximate deflected shape and the integration constants in the stress function are determined as follows:

First, only the nonperiodic terms for y are considered in pursuit of the condition of Eq.(B10), since the integral of the periodic terms for y over the circumference reduces to zero. Of course, this condition should be satisfied at any value of y .

Because only a locally deflected pattern and a rather long cylinder are considered, $e^{-\ell\beta L}$ can be put equal to zero. However, if the cylinder is short and the damping coefficient β is small, then the analytical results will lose their accuracy. If terms of $e^{-\ell\beta L}$ are neglected, the condition of Eq.(B10) can be written as

$$\sum_{\ell=1,2} \sum_{p=0,2} \alpha \left[(\mu B_{\ell po} - \ell \varphi A_{\ell po}) X_{\ell po,1} + (\mu A_{\ell po} + \ell \varphi B_{\ell po}) Y_{\ell po,1} \right] - \omega \left[\sum_{\ell=2,3,4} \sum_{p=0,2} \left((\mu B_{\ell po} - \ell \varphi A_{\ell po}) X_{\ell po,2} + (\mu A_{\ell po} + \ell \varphi B_{\ell po}) Y_{\ell po,2} \right) + \frac{3}{4\varphi} \xi \right] = 0 \quad (24)$$

Upon substitution of the values of $X_{\ell po,1}$, $Y_{\ell po,1}$; $X_{\ell po,2}$, $Y_{\ell po,2}$ in Eq.(24) and setting both terms of ω^0 and ω' equal to zero, ξ and δ can be written as functions of μ and φ only:

$$\left. \begin{aligned} \xi &= \frac{11}{72} - \frac{\varphi^4 (\mu^2 + 11\varphi^2)}{2(\mu^2 + \varphi^2)(4\mu^2 + 9\varphi^2)(\mu^2 + 4\varphi^2)} \\ \delta &= \frac{\varphi^4}{(4\mu^2 + \varphi^2)(\mu^2 + \varphi^2)} \end{aligned} \right\} \quad (25)$$

The remaining undetermined arbitrary parameters will be calculated through the use of the other boundary conditions for u , v and their derivatives. From Eq.(1), v_y can be given as follows:

$$\begin{aligned}
\frac{\partial v}{\partial y} &= \frac{\sigma_y}{E} - v \frac{\sigma_x}{E} - \frac{1}{2} \frac{w^2}{y} + \frac{w}{R} \\
&= v \left(\frac{\sigma}{E} \right) + (1+v)b^2 \sum_{r=2,4,\dots} C_r^2 e^{-rbx} \cos rby + (1+v)b^2 \sum_{s=1,3,\dots} C_s^2 e^{-sbx} \sin sby \\
&\quad + w \frac{t^2}{2} b^2 \sum_{\ell=1,2} \sum_{p_c=0,2} \sum_{q_c=0} e^{-\ell\beta x} \left[(J_{\ell pq}^X)_{\ell pq,1}^{-0} (J_{\ell pq}^Y)_{\ell pq,1} \cos pax + (O_{\ell pq}^X)_{\ell pq,1}^{+J} (Y_{\ell pq}^Y)_{\ell pq,1} \sin pax \right] \begin{matrix} \alpha \cos q_c by \\ (\sin q_s by) \end{matrix} \\
&\quad - w \frac{t^2}{2} b^2 \sum_{\ell=2,3,4} \sum_{p_c=0,2} \sum_{q_c=0,2} e^{-\ell\beta x} \left[X_{\ell pq,1} \rightarrow X_{\ell pq,2} \quad , \quad Y_{\ell pq,1} \rightarrow Y_{\ell pq,2} \right] \begin{matrix} \cos q_c by \\ (\alpha \sin q_s by) \end{matrix} \\
&\quad + w \frac{t^2}{2} b^2 \left[\left(e^{-\beta x} - \frac{1}{2} e^{-2\beta x} \right) \left(\alpha (\delta - \cos 2ax) + 2 \sin ax \sin by \right) + \gamma \right] \\
&\quad - \frac{1}{2} w \frac{t^2}{2} b^2 \left(e^{-2\beta x} - e^{-3\beta x} + \frac{1}{4} e^{-4\beta x} \right) (1 - \cos 2ax) (1 + \cos 2by) \\
&\quad - w \frac{t^2}{2} b^2 \sum_{\ell=2,3,4} Z_{\ell} e^{-\ell\beta x} (O_{\ell 11} \cos ax - J_{\ell 11} \sin ax) \sin by
\end{aligned} \tag{26}$$

where

$$\begin{aligned} J_{lpq} &= (p^2 \mu^2 - l^2 \varphi^2 - v q^2) A_{lpq} + 2 p l \mu \varphi B_{lpq} \\ O_{lpq} &= (p^2 \mu^2 - l^2 \varphi^2 - v q^2) B_{lpq} - 2 p l \mu \varphi A_{lpq} \end{aligned} \quad (27)$$

The condition of (B.11), that the displacement v must be a periodic function of y , leads to the determination of γ such that

$$v \frac{\sigma R}{E t} = - \omega \frac{\gamma}{\eta}, \quad (28)$$

since the terms which are nonperiodic in y and periodic in x become zero identically. It should be noted that γ is a constant, which means a uniform radial expansion due to a uniform axial stress. However, it is not an independent parameter in the case of the undamped, periodic deflected pattern discussed before⁵.

Integration of v_y with respect to y leads to

$$\begin{aligned} v &= (1+v) b \sum_{r=2,4,\dots} C_r e^{-r\beta x} \sin rby - (1+v) b \sum_{s=1,3} C_s e^{-s\beta x} \cos sby \\ &- \omega \frac{t^2}{\eta} b \sum_{l=1,2} \sum_{p_s=1} \sum_{q_s=1} \frac{1}{q} e^{-l\beta x} \\ &\times \left\{ (J_{lpq} X_{lpq,1} - O_{lpq} Y_{lpq,1}) \cos pax + (O_{lpq} X_{lpq,1} + J_{lpq} Y_{lpq,1}) \sin pax \right\} (-\cos q_s by) \\ &- \omega^2 \frac{t^2}{\eta} b \sum_{l=2,3,4} \sum_{p_c=0,2} \sum_{q_c=2} \frac{1}{q} e^{-l\beta x} \left\{ X_{lpq,1} \rightarrow X_{lpq,2}, Y_{lpq,1} \rightarrow Y_{lpq,2} \right\} \\ &\quad \sin q_c by \\ &\quad \times (-\alpha \cos q_s by) \end{aligned}$$

$$\begin{aligned}
& - \omega \frac{t^2}{\eta^2} b (2e^{-\beta x} - e^{-2\beta x}) \sin ax \cos by \\
& - \frac{1}{4} \omega^2 \frac{t^2}{\eta^2} b (e^{-2\beta x} - e^{-3\beta x} + \frac{1}{4} e^{-4\beta x}) \sin 2by \\
& + \omega^3 \frac{t^2}{\eta^2} b \xi \varphi^2 \sum_{\ell=2,3,4} Z_{\ell} e^{-\ell\beta x} (O_{\ell 11} \cos ax - J_{\ell 11} \sin ax) \cos by \quad (29)
\end{aligned}$$

In order to satisfy the boundary condition of Eq.(B.6), the terms in $\cos sby$ ($s=1,3,\dots$) should vanish, since the terms of $\sin rby$ ($r=2,4,\dots$) satisfy that condition identically. From this condition, the following relation can be obtained:

$$\left. \begin{aligned}
C_s &= 0 \quad (s = 3, 5, \dots) \\
- (1+\nu)C_1 &= \omega \frac{t^2}{\eta^2} \left\{ \sum_{\ell=1,2} (J_{\ell 11} X_{\ell 11,1} - O_{\ell 11} Y_{\ell 11,1}) - \alpha \omega \sum_{\ell=2,3,4} \sum_{p_s=1,3} \right. \\
& \quad \times (J_{\ell p 1} X_{\ell p 1,2} - O_{\ell p 1} Y_{\ell p 1,2}) - \omega^2 \xi \varphi^2 \sum_{\ell=2,3,4} Z_{\ell} O_{\ell 11} \left. \right\} \quad (30)
\end{aligned} \right\}$$

Next, from Eq.(1), u_x can be written as

$$\begin{aligned}
\frac{\partial u}{\partial x} &= \frac{\sigma_x}{E} - \nu \frac{\sigma_y}{E} - \frac{1}{2} \frac{w_x^2}{E} \\
&= -\frac{\sigma}{E} - (1+\nu) b^2 \sum_{r=2,4,\dots} C_r^2 e^{-r\beta x} \cos rby + \nu \omega^2 \frac{t^2}{2} \xi b^2 (e^{-\beta x} - \frac{1}{2} e^{-2\beta x}) - (1+\nu) b^2 C_1^2 e^{-\beta x} \sin by \\
&\quad - \omega^2 \frac{t^2}{2} \xi \varphi b^2 \sum_{\ell=2,3,4} Z_{\ell} e^{-\ell\beta x} (N_{\ell 11} \cos ax - M_{\ell 11} \sin ax) \sin by \\
&\quad + \omega^2 \frac{t^2}{2} b^2 \sum_{\ell=1,2} \sum_{p_c=0,2} \sum_{q_c=0} e^{-\ell\beta x} \left\{ (M_{\ell pq}^X \ell pq,1 - N_{\ell pq}^Y \ell pq,1) \cos pax + (N_{\ell pq}^X \ell pq,1 + M_{\ell pq}^Y \ell pq,1) \sin pax \right\} \begin{matrix} \alpha \cos q_c by \\ (\sin q_s by) \end{matrix} \\
&\quad - \omega^2 \frac{t^2}{2} b^2 \sum_{\ell=2,3,4} \sum_{p_c=0,2} \sum_{q_c=0,2} e^{-\ell\beta x} \left\{ X_{\ell pq,1} \rightarrow X_{\ell pq,2} \quad , \quad Y_{\ell pq,1} \rightarrow Y_{\ell pq,2} \right\} \begin{matrix} \cos q_c by \\ (\alpha \sin q_s by) \end{matrix} \\
&\quad - \frac{1}{8} \omega^2 \frac{t^2}{2} b^2 \sum_{\ell=2,3,4} \sum_{p_c=0,2,4} \sum_{q_c=0,2} e^{-\ell\beta x} (U_{\ell pq,2} \cos pax + W_{\ell pq,2} \sin pax) \begin{matrix} \cos q_c by \\ (\alpha \sin q_s by) \end{matrix} \\
&\quad + \omega^2 \frac{t^2}{2} b^2 \xi \varphi \sum_{\ell=2,3,4} \sum_{p_c=0,2} \sum_{q_c=0} e^{-\ell\beta x} (U_{\ell pq,3} \cos pax + W_{\ell pq,3} \sin pax) \begin{matrix} \alpha \cos q_c by \\ (\sin q_s by) \end{matrix} \\
&\quad - \frac{1}{2} \omega^2 \frac{t^2}{2} \xi b^2 \varphi^2 (e^{-2\beta x} - 2e^{-3\beta x} + e^{-4\beta x})
\end{aligned}
\tag{31}$$

where

$$\begin{aligned} M_{\ell pq} &= \left\{ q^2 - v(p^2 \mu^2 - \ell^2 \varphi^2) \right\} A_{\ell pq} - 2vp\ell\mu\varphi B_{\ell pq} \\ N_{\ell pq} &= \left\{ q^2 - v(p^2 \mu^2 - \ell^2 \varphi^2) \right\} B_{\ell pq} + 2vp\ell\mu\varphi A_{\ell pq} \end{aligned} \quad (32)$$

and

$$\begin{aligned} U_{202,2} &= -4(\mu^2 + \varphi^2), & U_{222,2} &= -4(\mu^2 - \varphi^2), & W_{222,2} &= 8\mu\varphi \\ U_{302,2} &= 4(\mu^2 + 2\varphi^2), & U_{322,2} &= 4(\mu^2 - 2\varphi^2), & W_{322,2} &= -12\mu\varphi \\ U_{402,2} &= -(\mu^2 + 4\varphi^2), & U_{422,2} &= -(\mu^2 - 4\varphi^2), & W_{422,2} &= 4\mu\varphi \\ U_{211,2} &= -8(1+2\delta)\mu\varphi, & U_{231,2} &= 24\mu\varphi, & U_{211,3} &= 2\mu \\ U_{311,2} &= 12(1+2\delta)\mu\varphi, & U_{331,2} &= -36\mu\varphi, & U_{311,3} &= -3\mu \\ U_{411,2} &= -4(1+2\delta)\mu\varphi, & U_{431,2} &= 12\mu\varphi, & U_{411,3} &= \mu \end{aligned} \quad (33)$$

In order to satisfy the boundary condition of Eq.(B.7), the terms of \sin by should vanish since the terms of $\cos r$ by ($r=0,2,\dots$) satisfy that condition identically. From this condition, the following relation can be obtained, since $\sum_{\ell=2,3,4} \sum_{p=1,3} U_{\ell p 1,2} = 0$ and $\sum_{\ell=2,3,4} U_{\ell 11,3} = 0$:

$$\begin{aligned} (1+v)C_1 &= \omega \frac{t^2}{\eta} \left[\sum_{\ell=1,2} (M_{\ell 11} X_{\ell 11,1} - N_{\ell 11} Y_{\ell 11,1}) \right. \\ &\quad - \alpha \omega \sum_{\ell=2,3,4} \sum_{p=1,3} (M_{\ell p 1} X_{\ell p 1,2} - N_{\ell p 1} Y_{\ell p 1,2}) \\ &\quad \left. - \xi \omega^2 \varphi^2 \sum_{\ell=2,3,4} Z_{\ell} N_{\ell 11} \right] \end{aligned} \quad (34)$$

From the conditions of Eqs.(30) and (34), the following equation can be obtained by eliminating C_1 :

$$\alpha\omega = -g(\mu,\varphi) - \omega^2 \xi k(\mu,\varphi) \quad (35)$$

where

$$g(\mu,\varphi) = - \frac{\sum_{\ell=1,2} (P_{\ell 11} X_{\ell 11,1} - Q_{\ell 11} Y_{\ell 11,1})}{\sum_{\ell=2,3,4} \sum_{p=1,3} (P_{\ell p 1} X_{\ell p 1,2} - Q_{\ell p 1} Y_{\ell p 1,2})} \quad (36)$$

$$k(\mu,\varphi) = \frac{\varphi^2 \sum_{\ell=2,3,4} Z_{\ell} Q_{\ell 11}}{\sum_{\ell=2,3,4} \sum_{p=1,3} (P_{\ell p 1} X_{\ell p 1,2} - Q_{\ell p 1} Y_{\ell p 1,2})}$$

Then, C_1 is given by

$$(1+v)C_1 = \frac{t^2}{\eta^2} (V\omega + T\omega^3)$$

where

$$V = I + Jg$$

$$T = \xi (Jk - M)$$

$$I(\mu,\varphi) = \sum_{\ell=1,2} (M_{\ell 11} X_{\ell 11,1} - N_{\ell 11} Y_{\ell 11,1}) \quad (38)$$

$$J(\mu,\varphi) = \sum_{\ell=2,3,4} \sum_{p=1,3} (M_{\ell p 1} X_{\ell p 1,2} - N_{\ell p 1} Y_{\ell p 1,2})$$

$$M(\mu,\varphi) = \varphi^2 \sum_{\ell=2,3,4} Z_{\ell} N_{\ell 11}$$

Integration of u_x with respect to x leads to

$$\begin{aligned}
u = & C_a - \frac{a}{E} x + (1+\nu)b \sum_{r=2,4,\dots} C_r e^{-rbx} \cos rby + (1+\nu)b C_1 e^{-bt} \sin by - \nu \omega^2 \frac{t^2}{2} \xi \frac{b}{\eta} (e^{-\beta x} - \frac{1}{4} e^{-2\beta x}) \\
& - \omega^3 \frac{t^2}{2} \xi \varphi^2 b \sum_{\ell=2,3,4} \sum_{\substack{p_c=0,2 \\ (p_s=1)}} \frac{Z_\ell e^{-\ell\beta x}}{(\mu^2 + \ell^2 \varphi^2)} \left[(\mu M_{\ell 11} - \ell \varphi N_{\ell 11}) \cos ax + (\mu N_{\ell 11} + \ell \varphi M_{\ell 11}) \sin ax \right] \sin by \\
& + \omega \frac{t^2}{2} b \sum_{\ell=1,2} \sum_{\substack{p_c=0,2 \\ (p_s=1)}} \sum_{q_c=0} \sum_{q_s=1} \frac{e^{-\ell\beta x}}{(\mu^2 + \ell^2 \varphi^2)} \left[- \left\{ (\ell \varphi M_{\ell pq} + \mu N_{\ell pq}) X_{\ell pq,1} + (\mu M_{\ell pq} - \ell \varphi N_{\ell pq}) Y_{\ell pq,1} \right\} \cos pax \right. \\
& \left. + \left\{ (\mu M_{\ell pq} - \ell \varphi N_{\ell pq}) X_{\ell pq,1} - (\mu N_{\ell pq} + \ell \varphi M_{\ell pq}) Y_{\ell pq,1} \right\} \sin pax \right] \alpha \cos q_c by \\
& \quad (\sin q_s by) \\
& - \omega^2 \frac{t^2}{2} b \sum_{\ell=2,3,4} \sum_{\substack{p_c=0,2 \\ (p_s=1,3)}} \sum_{q_c=0,2} \sum_{q_s=1} \frac{e^{-\ell\beta x}}{(\mu^2 + \ell^2 \varphi^2)} \left[X_{\ell pq,1} \rightarrow X_{\ell pq,2} \quad , \quad Y_{\ell pq,1} \rightarrow Y_{\ell pq,2} \right] \cos q_c by \\
& \quad (\alpha \sin q_s by) \\
& - \frac{1}{8} \omega^2 \frac{t^2}{2} b \sum_{\ell=2,3,4} \sum_{\substack{p_c=0,2,4 \\ (p_s=1,3)}} \sum_{q_c=0,2} \sum_{q_s=1} \frac{e^{-\ell\beta x}}{(\mu^2 + \ell^2 \varphi^2)} \left[- (\mu W_{\ell pq,2} + \ell \varphi U_{\ell pq,2}) \cos pax + (\mu U_{\ell pq,2} - \ell \varphi W_{\ell pq,2}) \sin pax \right] \\
& \quad \cos q_c by \\
& \quad \times (\alpha \sin q_s by) \\
& + \omega^3 \frac{t^2}{2} \xi \varphi^2 b \sum_{\ell=2,3,4} \sum_{\substack{p_c=0,2 \\ (p_s=1)}} \sum_{q_c=0} \sum_{q_s=1} \frac{e^{-\ell\beta x}}{(\mu^2 + \ell^2 \varphi^2)} \left[U_{\ell pq,2} \rightarrow U_{\ell pq,3} \quad , \quad W_{\ell pq,2} \rightarrow W_{\ell pq,3} \right] \alpha \cos q_c by \\
& \quad (\sin q_s by) \\
& + \frac{1}{2} \omega^4 \frac{t^2}{2} \xi \varphi^2 b \left(\frac{1}{2} e^{-2\beta x} - \frac{2}{3} e^{-3\beta x} + \frac{1}{4} e^{-4\beta x} \right)
\end{aligned} \tag{39}$$

The integral constant C_a can be determined so that the constant terms in $y(q_c=0)$ will be zero at $x = 0$.

In order to satisfy the boundary condition of Eq.(B.5),

$$C_r = 0 \quad (r \geq 4, 6, \dots) \quad (40)$$

and the terms of $\cos 2by$ ($r, q_c=2$) should be zero, since the terms of $\sin by$ satisfy this condition identically. From this condition, C_2 can be determined as follows without including α , δ and γ , which are not included in $X_{lp2,2}$, $U_{lp2,2}$ and $W_{lp2,2}$:

$$2(1+\nu)C_2 = -\omega^2 \frac{t^2}{\eta^2} \sum_{l=2,3,4} \sum_{p=0,2} \frac{1}{(p^2\mu^2 + l^2\varphi^2)} \left\{ (l\varphi M_{lp2} + p\mu N_{lp2}) X_{lp2,2} + \frac{1}{8} (U_{lp2,2} + W_{lp2,2}) \right\} \quad (41)$$

Consequently, all the arbitrary coefficients in the expression for w and all the integration constants in the expression of the stress function are determined as functions of ω , η , μ and φ . Thus, the damped diamond-shaped deflection pattern w is finally given by

$$\frac{w}{t} = -\nu \left(\frac{\sigma R}{Et} \right) + \frac{1}{\eta} \left(e^{-\beta x} - \frac{1}{2} e^{-2\beta x} \right) \left[(e+f\omega^2) + (g+h\omega^2) \cos 2ax + 2\omega \sin ax \sin by \right] \quad (42)$$

in which $e = -\delta g$, $f = \xi - h\delta$, $h = \xi k$

ξ , δ are given by Eq.(25) and k and g are given by Eq.(32). Because e , f , g and h are all functions of μ and φ only, it is convenient to use this new nondimensional expression for w to obtain the energy expression. With the use of this expression for w , $\nabla^4_{F/E}$ of Eq.(19) is expressed by the sum of the terms of ω as follows:

$$\begin{aligned}
\frac{\nabla^4 F}{E} = & \frac{t^2}{2} \frac{b^4}{\eta} \left[\sum_{\ell=1-4} \sum_{p=0,2} \sum_{m=0,2} e^{-\ell \beta x} \omega^m (R_{\ell p 0, m} \cos pax + S_{\ell p 0, m} \sin pax) \right. \\
& + \sum_{\ell=1-4} \sum_{p=1,3} \sum_{m=1,3} e^{-\ell \beta x} \omega^m (R_{\ell p 1, m} \cos pax + S_{\ell p 1, m} \sin pax) \sin by \\
& \left. + \sum_{\ell=2-4} \sum_{p=0,2} e^{-\ell \beta x} \omega^2 (R_{\ell p 2, 2} \cos pax + S_{\ell p 2, 2} \sin pax) \cos 2by \right]
\end{aligned} \tag{19a}$$

Then the stress components can be rewritten as

$$\begin{aligned}
\sigma_x = & \frac{F}{E} \frac{\partial^2}{\partial y^2} = - \left(\frac{\sigma}{E} \right) - 4 C_2 b^2 e^{-2 \beta x} \cos 2by - C_1 b^2 e^{-bx} \sin by \\
- & \frac{t^2}{2} \frac{b^2}{\eta} \sum_{\ell=1-4} \sum_{p=1,3} \sum_{m=1,3} e^{-\ell \beta x} \omega^m \{ (A_{\ell p 1, m}^R - B_{\ell p 1, m}^R S_{\ell p 1, m}) \cos pax + (B_{\ell p 1, m}^R + A_{\ell p 1, m}^R S_{\ell p 1, m}) \sin pax \} \sin by \\
- & 4 \frac{t^2}{2} \frac{b^2}{\eta} \sum_{\ell=2-4} \sum_{p=0,2} e^{-\ell \beta x} \omega^2 \{ (A_{\ell p 2, 2}^R - B_{\ell p 2, 2}^R S_{\ell p 2, 2}) \cos pax + (B_{\ell p 2, 2}^R + A_{\ell p 2, 2}^R S_{\ell p 2, 2}) \sin pax \} \cos 2by
\end{aligned} \tag{43a}$$

$$-\frac{\tau}{E} \frac{x y}{E} = \frac{F}{E} \frac{x y}{E} = 4C_2 b^2 e^{-2bx} \sin 2by - C_1 b^2 e^{-bx} \cos by$$

$$+ \frac{t^2}{\eta} b^2 \sum_{\ell=1-4} \sum_{p=1,3} \sum_{m=1,3} e^{-\ell \beta x} \omega^m \left\{ \begin{aligned} & \left[(\mu B_{\ell p 1} - \ell \varphi A_{\ell p 1}) R_{\ell p 1, m} + (\mu A_{\ell p 1} + \ell \varphi B_{\ell p 1}) S_{\ell p 1, m} \right] \cos pax \\ & - \left[(\mu A_{\ell p 1} + \ell \varphi B_{\ell p 1}) R_{\ell p 1, m} + (\ell \varphi A_{\ell p 1} - \mu B_{\ell p 1}) S_{\ell p 1, m} \right] \sin pax \end{aligned} \right\} \cos by$$

$$- 2 \frac{t^2}{\eta} b^2 \sum_{\ell=2-4} \sum_{p=0,2} e^{-\ell \beta x} \omega^2 \left\{ \begin{aligned} & A_{\ell p 1} \rightarrow A_{\ell p 2}, \quad B_{\ell p 1} \rightarrow B_{\ell p 2}, \quad R_{\ell p 1, m} \rightarrow R_{\ell p 2, m}, \quad S_{\ell p 1, m} \rightarrow S_{\ell p 2, m} \\ & \sin 2by \end{aligned} \right\} \quad (43b)$$

$$\frac{\sigma_y}{E} = \frac{F}{E} \frac{xx}{E} = 4C_2 b^2 e^{-2bx} \cos 2by + C_1 b^2 e^{-bx} \sin by$$

$$- \frac{t^2}{\eta} b^2 \sum_{\ell=1-4} \sum_{p=0,2} \sum_{m=0,2} e^{-\ell \beta x} \omega^m \left\{ \begin{aligned} & \left(\left[(p \mu^2 - \ell^2 \varphi^2) A_{\ell p 0} + 2p \ell \mu \varphi B_{\ell p 0} \right] R_{\ell p 0, m} - \left[(p \mu^2 - \ell^2 \varphi^2) B_{\ell p 0} - 2p \ell \mu \varphi A_{\ell p 0} \right] S_{\ell p 0, m} \right) \cos pax \\ & + \left(\left[(p \mu^2 - \ell^2 \varphi^2) B_{\ell p 0} - 2p \ell \mu \varphi A_{\ell p 0} \right] R_{\ell p 0, m} + \left[(p \mu^2 - \ell^2 \varphi^2) A_{\ell p 0} + 2p \ell \mu \varphi B_{\ell p 0} \right] S_{\ell p 0, m} \right) \sin pax \end{aligned} \right\}$$

$$- \frac{t^2}{\eta} b^2 \sum_{\ell=1-4} \sum_{p=1,3} \sum_{m=1,3} e^{-\ell \beta x} \omega^m \left\{ \begin{aligned} & A_{\ell p 0} \rightarrow A_{\ell p 1}, \quad B_{\ell p 0} \rightarrow B_{\ell p 1}, \quad R_{\ell p 0, m} \rightarrow R_{\ell p 1, m}, \quad S_{\ell p 0, m} \rightarrow S_{\ell p 1, m} \\ & \sin by \end{aligned} \right\}$$

$$- \frac{t^2}{\eta} b^2 \sum_{\ell=2-4} \sum_{p=0,2} e^{-\ell \beta x} \omega^2 \left\{ \begin{aligned} & A_{\ell p 0} \rightarrow A_{\ell p 2}, \quad B_{\ell p 0} \rightarrow B_{\ell p 2}, \quad R_{\ell p 0, m} \rightarrow R_{\ell p 2, 2}, \quad S_{\ell p 0, m} \rightarrow S_{\ell p 2, 2} \\ & \cos 2by \end{aligned} \right\} \quad (43c)$$

8. DETERMINATION OF POSTBUCKLING BEHAVIOR

The remaining deflection parameters, that is, μ , φ , ω and η , should be determined by means of the stationary energy theorem for the system. This condition can be enforced for $\sigma = \text{const.}$ or $\epsilon = \text{const.}$ for the cases of dead-weight loading and rigid testing machine loading, respectively. The total potential energy and the total strain energy are expressed as follows:

The extensional strain energy $W_1' = W_1 / (\pi t^3 E/R)$ is:

$$W_1' = \left(\frac{\sigma R}{E t} \right)^2 + \sqrt{\frac{R t}{L^2}} \eta^{-5/2} (\mathbb{K} + \omega^2 \mathbb{L} + \omega \mathbb{M} + \omega \mathbb{N}) \quad (44)$$

where

$$Y P(\ell_{i1}, \ell_{j1}, p_{i1}, p_{j1}, q_{i1}, m_{j1}) = \sum_{\ell_{i1}, \ell_{j1}} \sum_{\ell_{i2}, \ell_{j2}} \sum_{\ell_{j1} - \ell_{j2}} \sum_{p_{i1} - p_{i2}} \sum_{p_{j1} - p_{j2}} \sum_{p_{j1} - p_{j2}} Z P(\ell_i, \ell_j, p_i, p_j, q_i, m_j)$$

$$Z P(\ell_i, \ell_j, p_i, p_j, q_i, m_j) =$$

$$\begin{aligned} & \frac{1}{(p_i - p_j)^2 \mu^2 + (\ell_i + \ell_j)^2 \varphi^2} \left\{ \left[(\ell_i + \ell_j) \varphi^F \ell_i \ell_j p_i p_j q_i^{- (p_i - p_j) \mu G} \ell_i \ell_j p_i p_j q_i \right] \left({}^R \ell_i p_i q_i, m_i \ell_j p_j q_i, m_j + S \ell_i p_i q_i, m_i S \ell_j p_j q_i, m_j \right) \right\} \\ & - \left[(\ell_i + \ell_j) \varphi^G \ell_i \ell_j p_i p_j q_i^{+ (p_i - p_j) \mu F} \ell_i \ell_j p_i p_j q_i \right] \left({}^R \ell_i p_i q_i, m_i S \ell_j p_j q_i, m_j - S \ell_i p_i q_i, m_i {}^R \ell_j p_j q_i, m_j \right) \right\} \\ & + \frac{1}{(p_i + p_j)^2 \mu^2 + (\ell_i + \ell_j)^2 \varphi^2} \left\{ \left[(\ell_i + \ell_j) \varphi^H \ell_i \ell_j p_i p_j q_i^{+ (p_i + p_j) \mu I} \ell_i \ell_j p_i p_j q_i \right] \left({}^R \ell_i p_i q_i, m_i \ell_j p_j q_i, m_j - S \ell_i p_i q_i, m_i S \ell_j p_j q_i, m_j \right) \right\} \\ & - \left[(\ell_i + \ell_j) \varphi^I \ell_i \ell_j p_i p_j q_i^{- (p_i + p_j) \mu H} \ell_i \ell_j p_i p_j q_i \right] \left({}^R \ell_i p_i q_i, m_i S \ell_j p_j q_i, m_j + S \ell_i p_i q_i, m_i {}^R \ell_j p_j q_i, m_j \right) \right\} \quad (45) \end{aligned}$$

$$\begin{aligned}
F_{\ell, \ell, p, p, q} &= \left(P_{\ell, p, q}^P \ell_{j, p, q}^P + Q_{\ell, p, q}^Q \ell_{i, p, q}^Q \ell_{j, p, q}^Q \right)^{-2(1+\nu)} q^2 \left\{ \left(A_{\ell, p, q}^C \ell_{j, p, q}^{+B} \ell_{i, p, q}^D \ell_{j, p, q}^D \right) - \left(L_{\ell, p, q}^L \ell_{j, p, q}^{+K} \ell_{i, p, q}^K \ell_{j, p, q}^K \right) \right\} \\
G_{\ell, \ell, p, p, q} &= \left(P_{\ell, p, q}^Q \ell_{j, p, q}^Q - Q_{\ell, p, q}^Q \ell_{i, p, q}^P \ell_{j, p, q}^P \right)^{-2(1+\nu)} q^2 \left\{ \left(A_{\ell, p, q}^D \ell_{j, p, q}^{-B} \ell_{i, p, q}^C \ell_{j, p, q}^C \right) - \left(L_{\ell, p, q}^K \ell_{j, p, q}^{-K} \ell_{i, p, q}^K \ell_{j, p, q}^K \right) \right\} \\
H_{\ell, \ell, p, p, q} &= \left(P_{\ell, p, q}^P \ell_{j, p, q}^P - Q_{\ell, p, q}^Q \ell_{i, p, q}^Q \ell_{j, p, q}^Q \right)^{-2(1+\nu)} q^2 \left\{ \left(A_{\ell, p, q}^C \ell_{j, p, q}^{-B} \ell_{i, p, q}^D \ell_{j, p, q}^D \right) - \left(L_{\ell, p, q}^L \ell_{j, p, q}^{-K} \ell_{i, p, q}^K \ell_{j, p, q}^K \right) \right\} \\
I_{\ell, \ell, p, p, q} &= \left(P_{\ell, p, q}^Q \ell_{j, p, q}^Q + Q_{\ell, p, q}^Q \ell_{i, p, q}^P \ell_{j, p, q}^P \right)^{-2(1+\nu)} q^2 \left\{ \left(A_{\ell, p, q}^D \ell_{j, p, q}^{+B} \ell_{i, p, q}^C \ell_{j, p, q}^C \right) - \left(L_{\ell, p, q}^K \ell_{j, p, q}^{+K} \ell_{i, p, q}^K \ell_{j, p, q}^K \right) \right\}
\end{aligned} \tag{46}$$

$$\begin{aligned}
C_{\ell p q} &= (p^2 \mu^2 - \ell^2 \varphi^2) A_{\ell p q} + 2p\mu\varphi B_{\ell p q} , \\
D_{\ell p q} &= (p^2 \mu^2 - \ell^2 \varphi^2) B_{\ell p q} - 2p\mu\varphi A_{\ell p q} , \\
L_{\ell p q} &= p\mu B_{\ell p q} - \ell\varphi A_{\ell p q} , \\
K_{\ell p q} &= - (p\mu A_{\ell p q} + \ell\varphi B_{\ell p q}) , \\
P_{\ell p q} &= (p^2 \mu^2 - \ell^2 \varphi^2 + q^2) A_{\ell p q} + 2p\mu\varphi B_{\ell p q} = q^2 A_{\ell p q} + C_{\ell p q} , \\
Q_{\ell p q} &= (p^2 \mu^2 - \ell^2 \varphi^2 + q^2) B_{\ell p q} - 2p\mu\varphi A_{\ell p q} = q^2 B_{\ell p q} + D_{\ell p q} ,
\end{aligned} \tag{47}$$

$$\begin{aligned}
\textcircled{M1} &= \sum_{\ell=2,3,4} \sum_{p=0,2} \frac{1}{(p^2 \mu^2 + \ell^2 \varphi^2)} \left\{ (\ell \varphi^M_{\ell p 2} + p \mu^N_{\ell p 2}) X_{\ell p 2, 2} \right. \\
&\quad \left. + \frac{1}{8} (\ell \varphi^U_{\ell p 2, 2} + p \mu^W_{\ell p 2, 2}) \right\} \\
\textcircled{M2} &= \sum_{\ell=2,3,4} \sum_{p=0,2} \left\{ p \mu^B_{\ell p 2} - (\ell \varphi + 2) A_{\ell p 2} \right\} R_{\ell p 2, 2} \\
\textcircled{MS} &= \frac{2}{1+\nu} \textcircled{M1}^2 + 2 \textcircled{M1} \textcircled{M2}
\end{aligned} \tag{48}$$

$$\begin{aligned}
X_{202,2} = R_{202,2} = 2\mu^2, \quad X_{302,2} = R_{302,2} = -\frac{1}{2}(4\mu^2 - \varphi^2), \quad X_{402,2} = R_{402,2} = \frac{1}{2}\mu^2 \\
X_{322,2} = R_{322,2} = -\frac{1}{2}\varphi^2
\end{aligned} \tag{49}$$

$$\begin{aligned}
\textcircled{N1} &= \sum_{\ell=1-4} \sum_{p=1,3} \left\{ p \mu^B_{\ell p 1} - (\ell \varphi + 1) A_{\ell p 1} \right\} R_{\ell p 1, 1} + \left\{ p \mu^A_{\ell p 1} + (\ell \varphi + 1) B_{\ell p 1} \right\} S_{\ell p 1, 1} \\
\textcircled{N3} &= \sum_{\ell=1-4} \sum_{p=1,3} \left\{ p \mu^B_{\ell p 1} - (\ell \varphi + 1) A_{\ell p 1} \right\} R_{\ell p 1, 3} + \left\{ p \mu^A_{\ell p 1} + (\ell \varphi + 1) B_{\ell p 1} \right\} S_{\ell p 1, 3}
\end{aligned} \tag{50}$$

$$\begin{aligned}
V &= I + Jg, \quad T = \xi(Jk - M) \\
e &= -\delta g, \quad f = \xi - h\delta, \quad h = \xi k
\end{aligned} \tag{51}$$

$$\begin{aligned}
\xi &= \left(\frac{11}{72} \right) - \frac{\varphi^4 (\mu^2 + 11\varphi^2)}{2(\mu^2 + \varphi^2)(4\mu^2 + 9\varphi^2)(\mu^2 + 4\varphi^2)} \\
\delta &= \frac{\varphi^4}{(4\mu^2 + \varphi^2)(\mu^2 + \varphi^2)} \\
k &= \frac{\varphi^2 \sum_{\ell=2,3,4} Z_{\ell}^Q Q_{\ell 11}}{\sum_{\ell=2,3,4} \sum_{p=1,3} (P_{\ell p 1} X_{\ell p 1,2} - Q_{\ell p 1} Y_{\ell p 1,2})} = \frac{KN}{KD} \\
g &= \frac{- \sum_{\ell=1,2} (P_{\ell 11} X_{\ell 11,1} - Q_{\ell 11} Y_{\ell 11,1})}{\sum_{\ell=2,3,4} \sum_{p=1,3} (P_{\ell p 1} X_{\ell p 1,2} - Q_{\ell p 1} Y_{\ell p 1,2})} = \frac{GN}{KD} \\
I &= \sum_{\ell=1,2} (M_{\ell 11} X_{\ell 11,1} - N_{\ell 11} Y_{\ell 11,1}) \\
M &= \varphi^2 \sum_{\ell=2,3,4} Z_{\ell}^N N_{\ell 11} \\
J &= \sum_{\ell=2,3,4} \sum_{p=1,3} (M_{\ell p 1} X_{\ell p 1,2} - N_{\ell p 1} Y_{\ell p 1,2})
\end{aligned} \tag{52}$$

$$\begin{aligned}
\textcircled{LA} &= V \left(\frac{V}{1+v} - \textcircled{N1} \right) \\
\textcircled{MA} &= \frac{2VT}{1+v} - (T \textcircled{N1} + v \textcircled{N3}) \\
\textcircled{NA} &= T \left(\frac{T}{1+v} - \textcircled{N3} \right)
\end{aligned} \tag{53}$$

$$\textcircled{\text{K}} = \frac{1}{2} \text{YP} \begin{pmatrix} \ell_{i1}, \ell_{i2} & P_{i1}, P_{j1} & 0, 0, 0 \\ \ell_{j1}, \ell_{j2} & \underline{0,2}, \underline{0,2} & \\ 1-2, 1-2 & & \end{pmatrix}$$

$$\textcircled{\text{L}} = \frac{1}{2} \text{YP}(1-4, 1-4; \underline{0,2}, \underline{0,2}; 0; 0,2) + \frac{1}{2} \text{YP}(1-4, 1-4; \underline{0,2}, \underline{0,2}; 0; 2,0) \\ + \frac{1}{4} \text{YP}(1-4, 1-4; \underline{1,3}, \underline{1,3}; 1; 1,1) + \textcircled{\text{LA}}$$

$$\textcircled{\text{M}} = \frac{1}{2} \text{YP}(1-4, 1-4; \underline{0,2}, \underline{0,2}; 0; 2,2) \\ + \frac{1}{4} \text{YP}(1-4, 1-4; \underline{1,3}, \underline{1,3}; 1; 1,3) + \frac{1}{4} \text{YP}(1-4, 1-4; \underline{1,3}, \underline{1,3}; 1; 3,1) \\ + \frac{1}{4} \text{YP}(2-4, 2-4; \underline{0,2}, \underline{0,2}; 2; 2,2) + \textcircled{\text{MS}} + \textcircled{\text{MA}}$$

$$\textcircled{\text{N}} = \frac{1}{4} \text{YP}(1-4, 1-4; \underline{1,3}, \underline{1,3}; 1; 3,3) + \textcircled{\text{NA}}$$

$$\left(\begin{array}{lll} R_{100,0} = -e\varphi^2, & R_{120,0} = (4\mu^2 - \varphi^2)g, & S_{120,0} = -4\mu\varphi g \\ R_{100,2} = -f\varphi^2, & R_{120,2} = (4\mu^2 - \varphi^2)h, & S_{120,2} = -4\mu\varphi h \\ R_{11,1} = 4\mu\varphi, & S_{111,1} = 2(\mu^2 - \varphi^2) & \end{array} \right)$$

(54)

$$\begin{aligned}
& \left[\begin{aligned}
R_{200,0} &= 2e\varphi^2, \\
R_{200,2} &= 2(1+f)\varphi^2, \\
R_{211,1} &= -4\mu\varphi(1-g), \quad S_{211,1} = 2e\varphi^2 + (4\mu^2 - \varphi^2)g - (\mu^2 - 4\varphi^2), \\
R_{211,3} &= 4\mu\varphi h, \quad S_{211,3} = (4\mu^2 - \varphi^2)h + 2f\varphi^2, \\
R_{202,2} &= 2\mu^2
\end{aligned} \right. \\
& \left. \begin{aligned}
R_{220,0} &= -2(\mu^2 - \varphi^2)g, \quad S_{220,0} = 4\mu\varphi g \\
R_{220,2} &= 2(\mu^2 - \varphi^2)(1-h), \quad S_{220,2} = -4\mu\varphi(1-h) \\
R_{231,1} &= -4\mu\varphi g, \quad S_{231,1} = -(4\mu^2 - \varphi^2)g \\
R_{231,3} &= -4\mu\varphi h, \quad S_{231,3} = -(4\mu^2 - \varphi^2)h
\end{aligned} \right\} \quad (55) \\
& \left[\begin{aligned}
R_{300,2} &= -\frac{9}{2}\varphi^2, \\
R_{311,1} &= -6\mu\varphi g, \quad S_{311,1} = -\left[\frac{1}{2}(8\mu^2 - 5\varphi^2)g + 5e\varphi^2\right], \\
R_{311,3} &= -6\mu\varphi h, \quad S_{311,3} = -\left[\frac{1}{2}(8\mu^2 - 5\varphi^2)h + 5f\varphi^2\right], \\
R_{302,2} &= -\frac{1}{2}(4\mu^2 - \varphi^2),
\end{aligned} \right. \\
& \left. \begin{aligned}
R_{400,2} &= 2\varphi^2, \\
R_{411,1} &= 2\mu\varphi g, \quad S_{411,1} = (\mu^2 - \varphi^2)g + 2e\varphi^2, \\
R_{411,3} &= 2\mu\varphi h, \quad S_{411,3} = (\mu^2 - \varphi^2)h + 2f\varphi^2, \\
R_{402,2} &= \frac{1}{2}\mu^2
\end{aligned} \right\}
\end{aligned}$$

The bending strain energy $W'_2 = W_2/(\pi t^3 LE/R)$ is:

$$W'_2 = \sqrt{\frac{Rt}{L^2}} \eta^{-1/2} (\textcircled{H} + \omega^2 \textcircled{I} + \omega^4 \textcircled{J}) \quad (56)$$

$$\left[\begin{aligned} \textcircled{H} &= \frac{g^2}{12(1-\nu^2)\varphi} \left(\frac{1}{6} \delta^2 \varphi^4 - \delta \textcircled{A} + \textcircled{C} \right) \\ \textcircled{I} &= \frac{1}{12(1-\nu^2)\varphi} \left[\frac{1}{3} ef\varphi^2 + \frac{1}{48} (11\mu^4 + 8\varphi^4 + 24\mu^2\varphi^2 + 22\mu^2 + 8\varphi^2 + 11) \right. \\ &\quad \left. + (eh+fg)\textcircled{A} - \textcircled{B} + 2gh\textcircled{C} \right] \\ \textcircled{J} &= \frac{1}{12(1-\nu^2)\varphi} \left(\frac{1}{6} f^2 \varphi^4 + fh\textcircled{A} + h^2 \textcircled{C} \right) \end{aligned} \right] \quad (57)$$

$$\left[\begin{aligned} \textcircled{A} &= \varphi^4 \times \frac{12\mu^6 + 72\mu^4\varphi^2 + 57\mu^2\varphi^4 + 12\varphi^6}{(\mu^2 + \varphi^2)(4\mu^2 + 9\varphi^2)(\mu^2 + 4\varphi^2)} \\ \textcircled{B} &= \varphi^4 \times \frac{3(\mu^6 + 7\mu^4\varphi^2 + 14\mu^2\varphi^4 + 8\varphi^6 + 2\mu^4 + 10\mu^2\varphi^2 + 8\varphi^4 + \mu^2 + 11\varphi^2)}{4(\mu^2 + \varphi^2)(4\mu^2 + 9\varphi^2)(\mu^2 + 4\varphi^2)} \\ \textcircled{C} &= \varphi^4 \times \frac{3(2\mu^2 + \varphi^2)}{4(16\mu^2 + 9\varphi^2)} + \frac{22\mu^4 + 12\mu^2\varphi^2 + \varphi^4}{12} \end{aligned} \right] \quad (58)$$

The potential energy of the axial stress $W'_p = W_p/(\pi t^3 L E/R)$ is:

$$W'_p = -2 \left(\frac{\sigma R}{E t} \right)^2 - \sqrt{\frac{R t}{L^2}} \left(\frac{\sigma R}{E t} \right) \eta^{-3/2} (\textcircled{E} + \omega^2 \textcircled{F} + \omega^4 \textcircled{G}) \quad (59)$$

$$\left. \begin{aligned} \textcircled{E} &= \frac{g^2}{\varphi} \left\{ \textcircled{Z} \delta - \textcircled{V} \delta + \textcircled{W} \right\} \\ \textcircled{F} &= \frac{1}{\varphi} \left\{ \frac{\mu^2 (44\mu^2 + 115\varphi^2)}{48(4\mu^2 + 9\varphi^2)} + 2 \textcircled{Z} e f + 2 \textcircled{W} g h + \textcircled{V} (e h + f g) \right\} \\ \textcircled{G} &= \frac{1}{\varphi} \left\{ \textcircled{Z} f^2 + \textcircled{W} h^2 + \textcircled{V} f h \right\} \end{aligned} \right\} \quad (60)$$

$$\left. \begin{aligned} \textcircled{V} &= \frac{3\varphi^4 (\mu^4 + 8\mu^2 \varphi^2 + 2\varphi^4)}{(\mu^2 + \varphi^2)(4\mu^2 + 9\varphi^2)(\mu^2 + 4\varphi^2)} \\ \textcircled{W} &= \frac{176\mu^4 + 115\mu^2 \varphi^2 + 18\varphi^4}{24(16\mu^2 + 9\varphi^2)} \\ \textcircled{Z} &= \varphi^2/12 \end{aligned} \right\} \quad (61)$$

The unit end shortening of an axially compressed shell (ϵ) is the ratio of the total shortening in the axial direction to the length of the cylinder; it can be defined as

$$\epsilon = -\left(\frac{1}{L}\right) \int_0^L \left(\frac{\partial u}{\partial x}\right) dx \quad (62)$$

Through the use of Eqs.(1), (42) and (43), ϵ can be given by

$$\left(\epsilon \frac{R}{t}\right) = \left(\frac{\sigma R}{Et}\right) + \sqrt{\frac{Rt}{L^2}} \eta^{-3/2} \frac{\textcircled{E} + \omega^2 \textcircled{F} + \omega^4 \textcircled{G}}{2} \quad (63)$$

It can be seen from this equation that $\frac{\sqrt{Rt}}{L}$ enters into the relation between σ and ϵ ; this is different from the case of overall undamped buckling.

(1) First the case of dead-weight loading will be considered. The total potential energy W can be expressed in the nondimensional form as

$$W' = (W_1 + W_2 + W_p) / (\pi t^3 LE/R) = - \left(\frac{\sigma R}{Et}\right)^2 + \sqrt{\frac{Rt}{L^2}} W'_t \quad (64)$$

where

$$\left. \begin{aligned} W'_t &= \eta^{-5/2} \left\{ \textcircled{R} - \frac{\sigma R}{Et} \eta \textcircled{Q} + \eta^2 \textcircled{P} \right\} \\ \textcircled{R} &= \textcircled{K} + \omega^2 \textcircled{L} + \omega^4 \textcircled{M} + \omega^6 \textcircled{N} \\ \textcircled{Q} &= \textcircled{E} + \omega^2 \textcircled{F} + \omega^4 \textcircled{G} \\ \textcircled{P} &= \textcircled{H} + \omega^2 \textcircled{I} + \omega^4 \textcircled{J} \end{aligned} \right\} \quad (65)$$

In order to determine the postbuckling characteristics of the axially compressed shell, it is necessary to determine the deflection parameters μ , φ , ω and η from the condition that the total potential energy (W') of the system has a stationary value with respect to any small variation of the parameters.

W' is a simple function of ω and η , and so the following two equations can be easily obtained from the conditions of $(\partial W' / \partial \omega) = 0$ and $(\partial W' / \partial \eta) = 0$, respectively.

$$\textcircled{U} - \left(\frac{\sigma R}{Et}\right) \eta \textcircled{T} + \eta^2 \textcircled{S} = 0 \quad (66)$$

$$5 \textcircled{R} - 3 \left(\frac{\sigma R}{Et}\right) \eta \textcircled{Q} + \eta^2 \textcircled{P} = 0 \quad (67)$$

where

$$\left. \begin{aligned} \textcircled{U} &= \textcircled{L} + 2\omega^2 \textcircled{M} + 3\omega^4 \textcircled{N} \\ \textcircled{T} &= \textcircled{F} + 2\omega^2 \textcircled{G} \\ \textcircled{S} &= \textcircled{I} + 2\omega^2 \textcircled{J} \end{aligned} \right\} \quad (68)$$

However, since μ and φ appear in the expression for W' in a rather complicated manner, it is too difficult to get analytical expressions for $\partial W'/\partial \mu = 0$ and $\partial W'/\partial \varphi = 0$. These conditions can be expressed as

$$\frac{\partial}{\partial \mu} \left[\eta^{-5/2} \left\{ \textcircled{R} - \left(\frac{\sigma R}{Et}\right) \eta \textcircled{Q} + \eta^2 \textcircled{P} \right\} \right] = 0 \quad (69)$$

$$\frac{\partial}{\partial \varphi} \left[\eta^{-5/2} \left\{ \textcircled{R} - \left(\frac{\sigma R}{Et}\right) \eta \textcircled{Q} + \eta^2 \textcircled{P} \right\} \right] = 0 \quad (70)$$

As a principle of solution, the four deflection parameters can be determined from the above four nonlinear algebraic equations (66), (67), (69) and (70), under a constant value of σ and then a relation between $(\sigma R/Et)$ and ω can be obtained. This relation can be replaced by the load-deflection curve, $(\sigma R/Et)$ versus ϵ , by use of the relation of Eq.(63).

As stated above, W' is a very complicated function of μ and φ and so, for the numerical process, it is more expedient to fix μ and φ (under a specified value of ω) and then to solve for $(\sigma R/Et)$ along with the remaining deflection parameters, than it is to fix $(\sigma R/Et)$ and to solve for all the deflection parameters. That is to say, the following numerical successive approximation procedure will be used:

First, a set of values of μ and φ and a value of ω is assumed. Then, (R/Et) and η can be determined from Eqs.(66) and (67) as follows:

$$\eta_o^2 = - (Y/X) \quad (71)$$

$$\left(\frac{\sigma R}{Et}\right)_o = \frac{5(R) + \eta_o^2(P)}{3\eta_o(Q)} = \frac{\eta_o(S) + U/\eta_o}{T} \quad (72)$$

where

$$(X) = (P)(T) - 3(Q)(S) \quad , \quad (Y) = 5(R)(T) - 3(Q)(U) \quad (73)$$

Through use of these values of $(\sigma R/Et)_o$ and η_o , Wt' can be calculated for given values of ω , μ and φ . This procedure is repeated for several assumed values of ω and several sets of μ and φ . The particular set of μ , φ and $\omega(\eta)$ which minimizes the value of $W't$ for a fixed value of $(\sigma R/Et)$ is the one which we are looking for. Through changing the specified values of $(\sigma R/Et)$, the relationship between $(\sigma R/Et)$ and $(\epsilon R/t)$ can be obtained and plotted as a curve.

In this case, the length L of the cylinder has no effect on the deflected pattern and the postbuckling stress, but it has an effect on the load-shortening curve through Eq.(63) with a parameter of (\sqrt{Rt}/L) .

(2) The case of the rigid-testing-machine loading will now be considered. In this case, the sum of W_1 and W_2 , that is, the elastic strain energy should have a stationary value for a constant value of ϵ . Thus, $\delta W_p = 0$, since no axial displacements are permitted. $(W_1 + W_2)$ can be expressed in terms of ϵ rather than σ with the aid of Eq.(63) as follows:

$$W'' = (W_1 + W_2)/(\pi t^3 L E/R) = \left(\epsilon \frac{R}{t}\right)^2 + \sqrt{\frac{Rt}{L^2}} W_s'' \quad (74)$$

where

$$W_s'' = \eta^{-5/2} \left[\textcircled{R} - \left(\epsilon \frac{R}{t} \right) \eta \textcircled{Q} + \eta^2 \textcircled{P} + \frac{1}{4} \sqrt{\frac{Rt}{L^2}} \eta^{-1/2} \textcircled{Q}^2 \right]$$

In order to determine the postbuckling characteristics of the axially compressed shell in a rigid testing machine, the deflection parameters μ , φ , ω and η should be determined by the same process as described in (1), with the exception that $(\epsilon R/t)$ should be maintained constant instead of $(\sigma R/Et)$. Since W'' is a simple function of ω and η , the following two equations can be easily obtained from the condition of $(\partial W''/\partial \omega) = 0$ and $(\partial W''/\partial \eta) = 0$, respectively.

$$\eta^2 \textcircled{S} - \left(\epsilon \frac{R}{t} \right) \eta \textcircled{T} + \textcircled{U} + \sqrt{\frac{Rt}{L^2}} \frac{1}{2} \eta^{-1/2} \textcircled{Q} \textcircled{T} = 0 \quad (75)$$

$$\eta^2 \textcircled{P} - 3 \left(\epsilon \frac{R}{t} \right) \eta \textcircled{Q} + 5 \textcircled{R} + \sqrt{\frac{Rt}{L^2}} \frac{3}{2} \eta^{-1/2} \textcircled{Q}^2 = 0 \quad (76)$$

The value of η_0 can be given by eliminating $(\epsilon R/t)$ from both Eqs.(75) and (76):

$$\eta_0^2 = - \textcircled{Y} / \textcircled{X} \quad (71a)$$

This is the same as Eq.(71); and $(\epsilon R/t)$ is obtained from Eq.(75) as

$$\left(\epsilon \frac{R}{t} \right)_0 = \frac{\eta_0 \textcircled{S} + \frac{\textcircled{U}}{\eta_0}}{\textcircled{T}} + \sqrt{\frac{Rt}{L^2}} \eta^{-3/2} \frac{\textcircled{Q}}{2} \quad (77)$$

Next, $(\sigma R/Et)_0$ is given by

$$\left(\frac{\sigma R}{Et} \right)_0 = \frac{\eta_0 \textcircled{S} + \frac{\textcircled{U}}{\eta_0}}{\textcircled{T}} \quad (72a)$$

which is also the same as Eq.(72).

This means that both the case of dead-weight loading and the case of rigid-testing-machine loading lead to the same relationship between load and shortening under a specified value of (\sqrt{Rt}/L) .

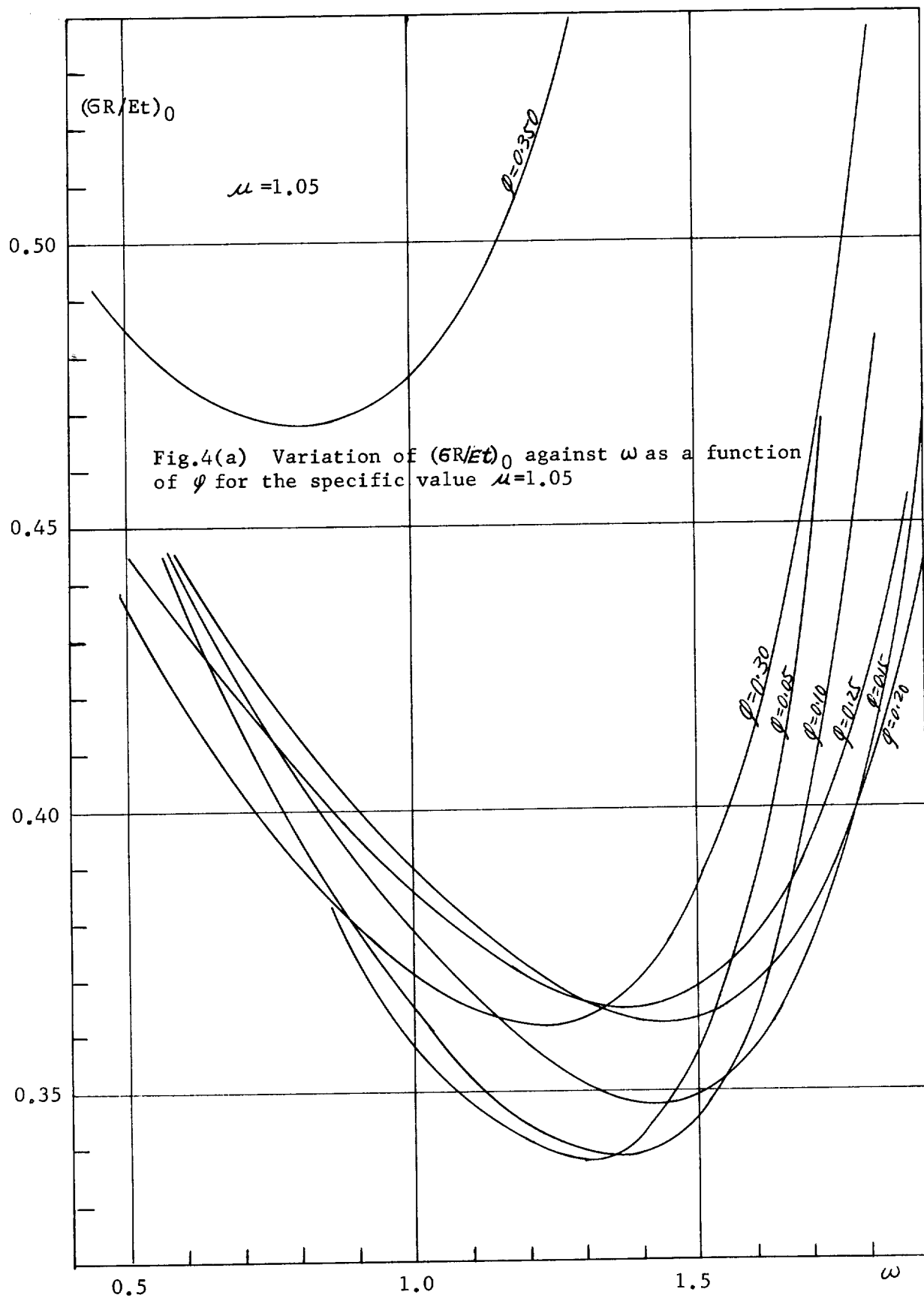
However, as stated before, the unit shortening $\epsilon R/t$ depends on the value of \sqrt{Rt}/L , and so the buckling stresses depend on (\sqrt{Rt}/L) under specified values of shortening. On the other hand, it has been pointed out in the many experimental reports, for example, those mentioned in reference [12] , that the buckling stresses for the case of rigid-testing-machine loading depend not only on the values of R/t , but also on those of L/t . This fact is verified by the above analytical results.

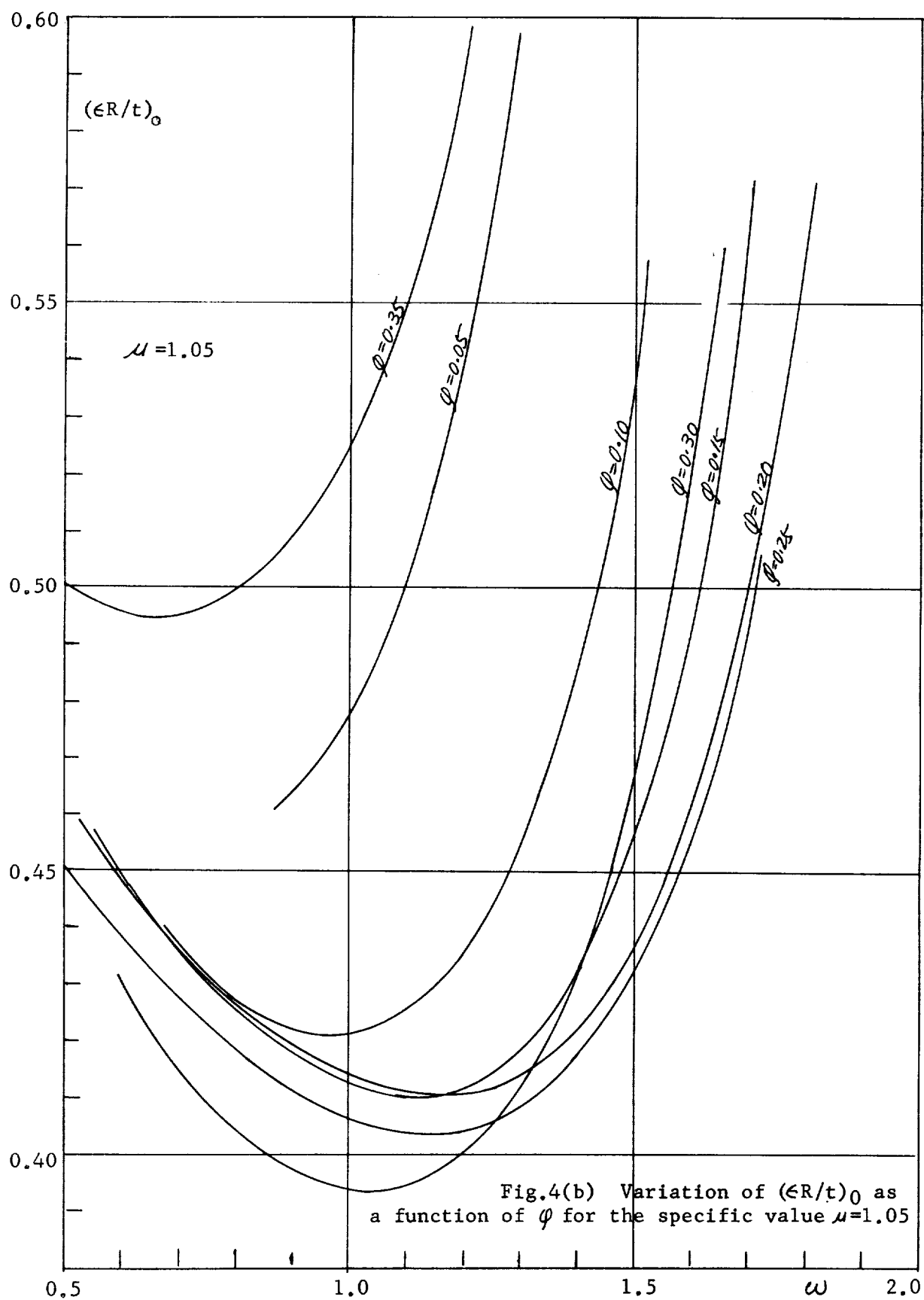
9. NUMERICAL RESULTS

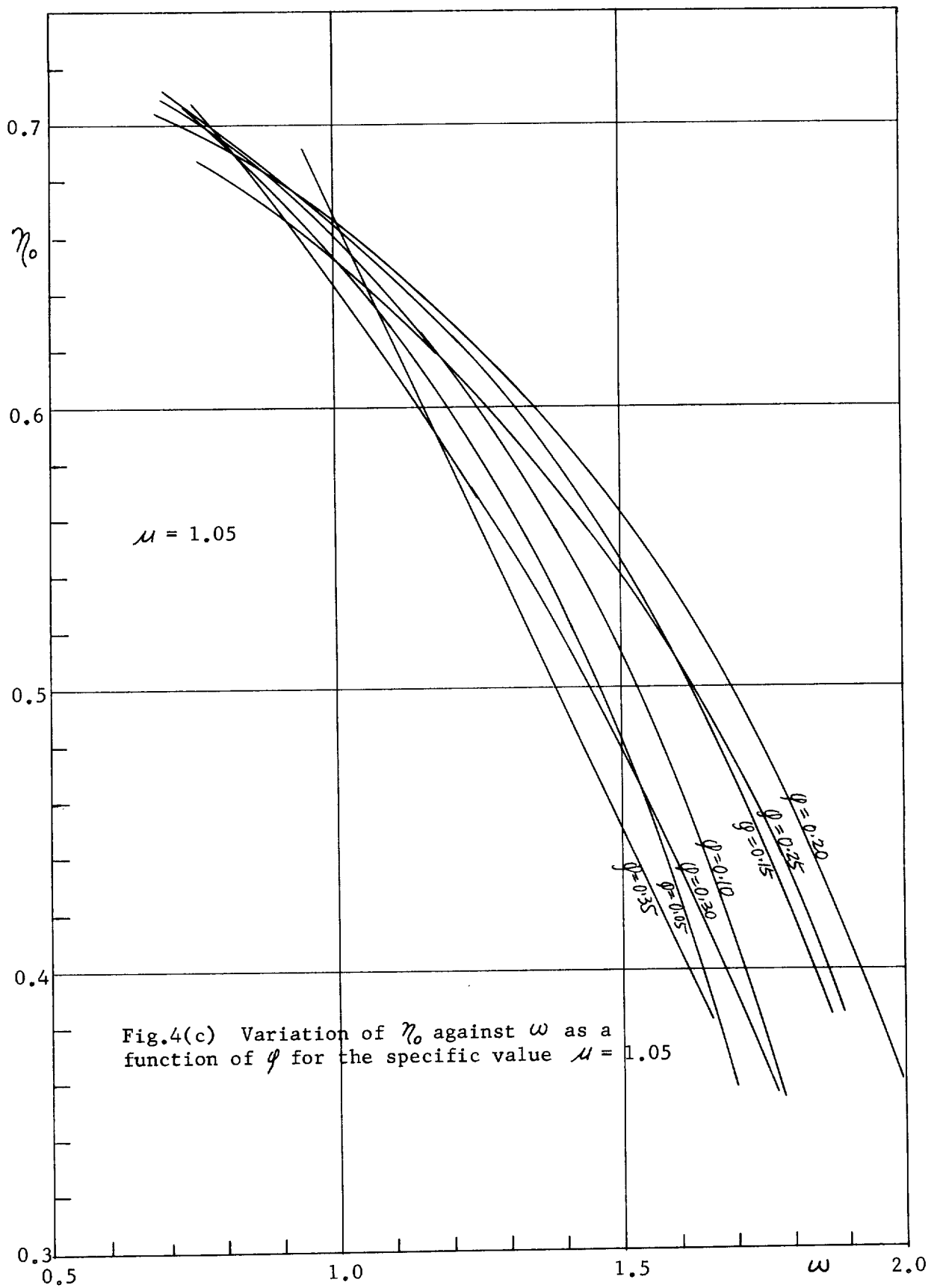
As was shown in the preceding chapter, the two cases of dead-weight loading and rigid-testing-machine loading give the same relationship between load and shortening. Accordingly, the equilibrium curves will now be obtained for the latter case of loading in a rigid testing machine. Most experiments have, of course, been performed in approximately-rigid testing machines, because a dead-weight loading condition would inevitably give large postbuckling deflections, which would result in plastic deformations and make it impossible to check the buckling mechanism.

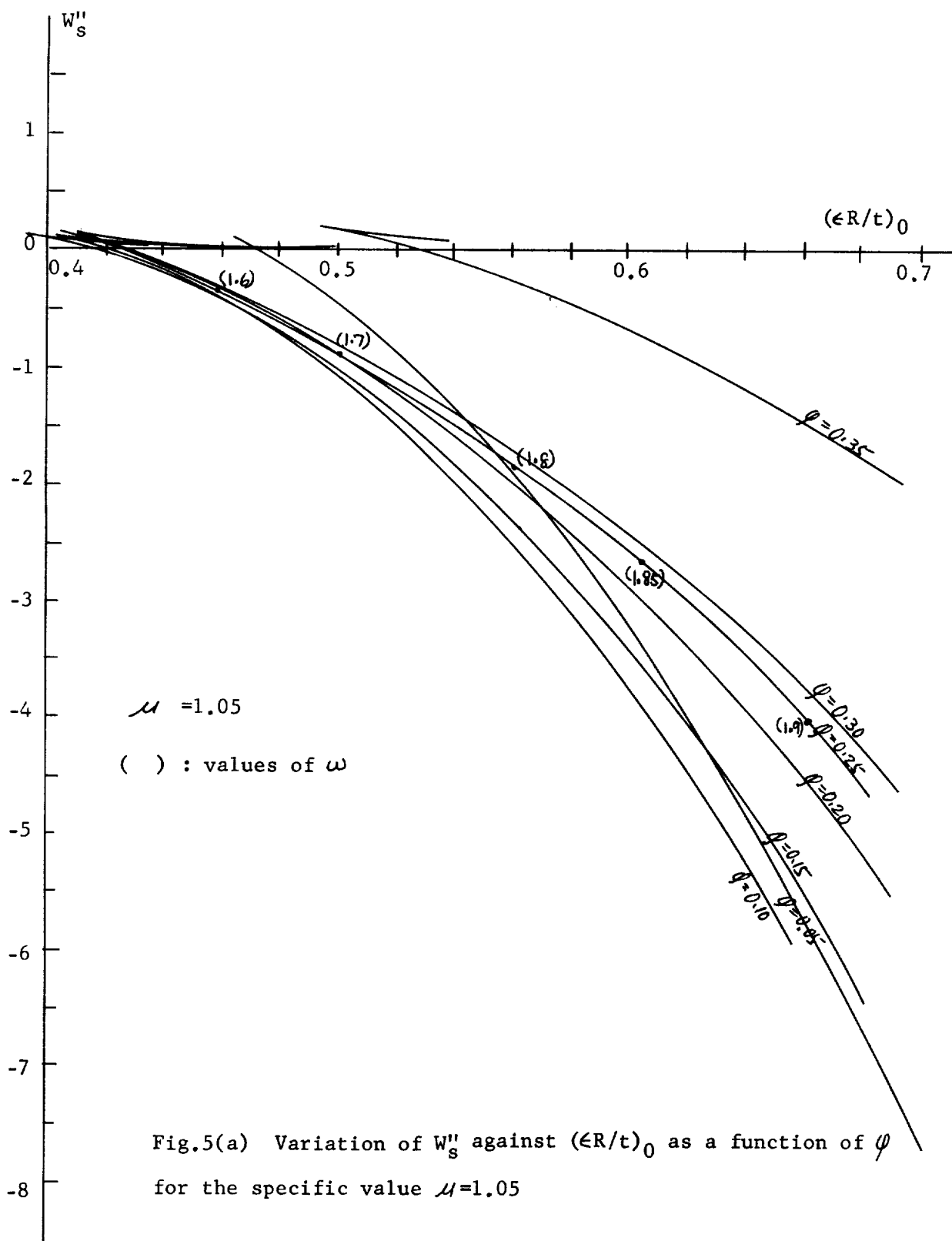
First, as an example, the variation of the calculated values of $(\sigma R/Et)_0$, $(\epsilon R/t)_0$ and η_0 against ω is shown in Figs.4(a), 4(b) and 4(c), respectively, for the case of $\mu = 1.05$. These curves were obtained from Eqs.(71), (62) and (72), respectively, by satisfying the minimum condition with respect to η and ω only. In the numerical calculation Poisson's ratio was set equal to 0.3 and the curvature ratio \overline{Rt}/L was set equal to 0.015 in the calculation of $\epsilon R/t$ (for this example). The effect of the curvature ratio Rt/L will be discussed later. Both of $(\sigma R/Et)_0$ and $(\epsilon R/t)_0$ have minimal values with respect to ω , which means that minimal values of these parameters exist in the postbuckling equilibrium states. Next, the variation of W_s'' against $(\epsilon R/t)_0$ as a parameter of ϕ is shown in Figs.5(a) and 5(b) for the same $\mu = 1.05$. Fig.5(b) is an enlargement of Fig.5(a) in the region of small values of $(\epsilon R/t)_0$. The values of ω on each curve are varying as shown in the parentheses on the curve of $\phi = 0.25$, for example. Each curve forms a cusp and it seems that the lower curve corresponds to stable equilibrium states, while the upper curve corresponds to unstable equilibrium states.

For the case of rigid-testing-machine loading, which is now considered, a value of $(\epsilon R/t)$ should be specified. The variation of W_s'' with respect to ϕ can be plotted as shown in Fig.6 for the specified value of $\epsilon R/t$ equal to 0.48, as an example. The values of W_s'' have some minimal values with respect to ϕ for a specified μ . This means that the damped deflection pattern exhibiting a local buckling pattern









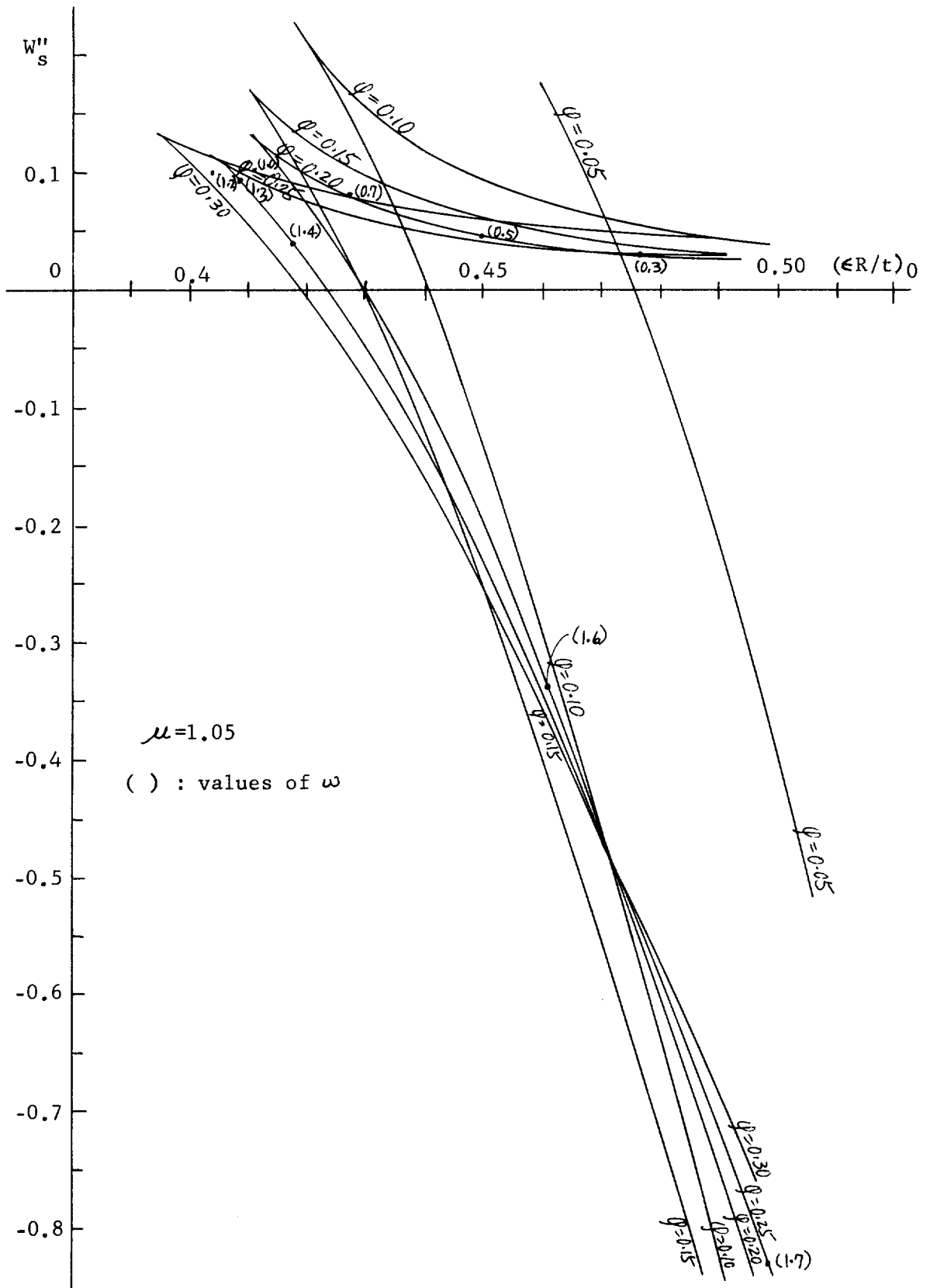


Fig.5(b) Enlargement of Fig.5(a) in the region of small $(\epsilon R/t)_0$

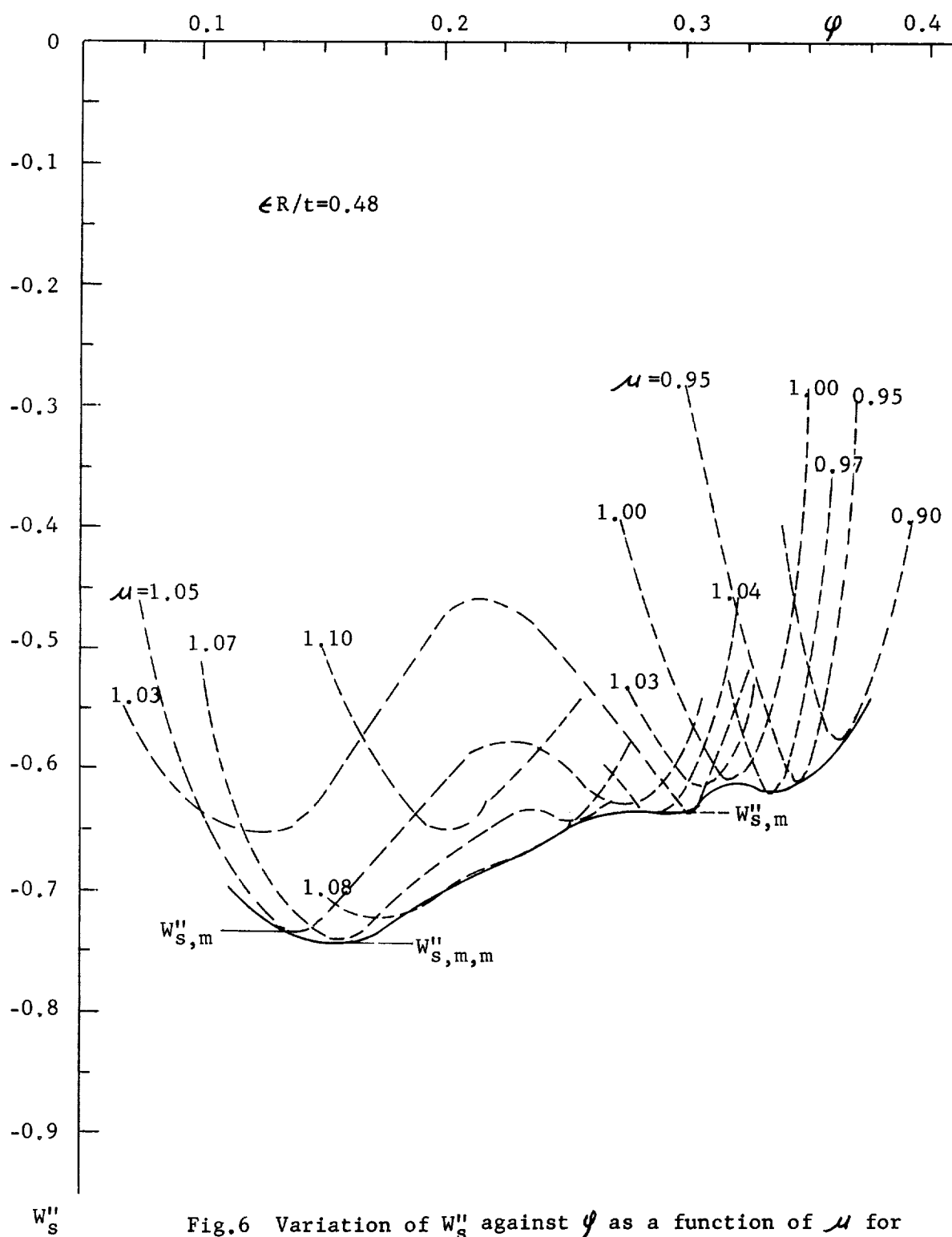


Fig.6 Variation of W''_s against ψ as a function of μ for the specific value $(\epsilon R/t)=0.48$

will be more reasonable than an overall sinusoidal pattern in the axial direction.

By repeating such a process for the other values of μ , a group of such curves can be obtained as seen in Fig.6. It is interesting to note that some curves for specified values of μ have more than one minimum point. Consequently, if the minimal values ($W''_{s,m}$) of these curves are plotted against μ , a few kinds of curves of $W''_{s,m}$ are obtained as seen in Fig.7. These local minima $W''_{s,m,m}$ shown by (I) and (II) in Fig.7 are the equilibrium points which satisfy the minimal conditions with respect to all the parameters μ , φ , η and ω under a specified value of $\epsilon R/t$. The fact that there are several local minima means that there are several possible equilibrium states under a specified shortening.

The values of $W''_{s,m,m}$ on the local minima of (I) and (II) are plotted in Fig.8. It seems that there are some other local minima in addition to (I) and (II); however, because of the viewpoint that the equilibrium state having the lowest value of $W''_{s,m,m}$ will be the most stable equilibrium state after buckling, only the lowest point was plotted in Fig.8. Other local minima having a higher level of energy were thus neglected. The lowest minimal point gives a point, under a specified value of $(\epsilon R/t)$, on the load-shortening curve of Fig.9.

By specifying other values of $(\epsilon R/t)$, the lowest minima yield the postbuckling equilibrium curve in question shown in Fig.9. The values of φ_m , μ_m , η_m and ω_m corresponding to these equilibrium states are plotted in Figs.10, 11, 12 and 13, respectively.

As φ becomes smaller along curve (II), the analysis loses its accuracy because $e^{-\ell\beta L}$ ($e^{-\ell\varphi bL}$) was set equal to zero on the assumption that the length of cylinder L or the damping coefficient φ is not too small. Accordingly, the equilibrium curve in the region of larger $(\epsilon R/t)$ has been omitted here.

In the case of dead-weight loading, the same process can be used with the exception that W''_s and $\epsilon R/t$ should be replaced by W'_t and $(\sigma R/Et)$, respectively.

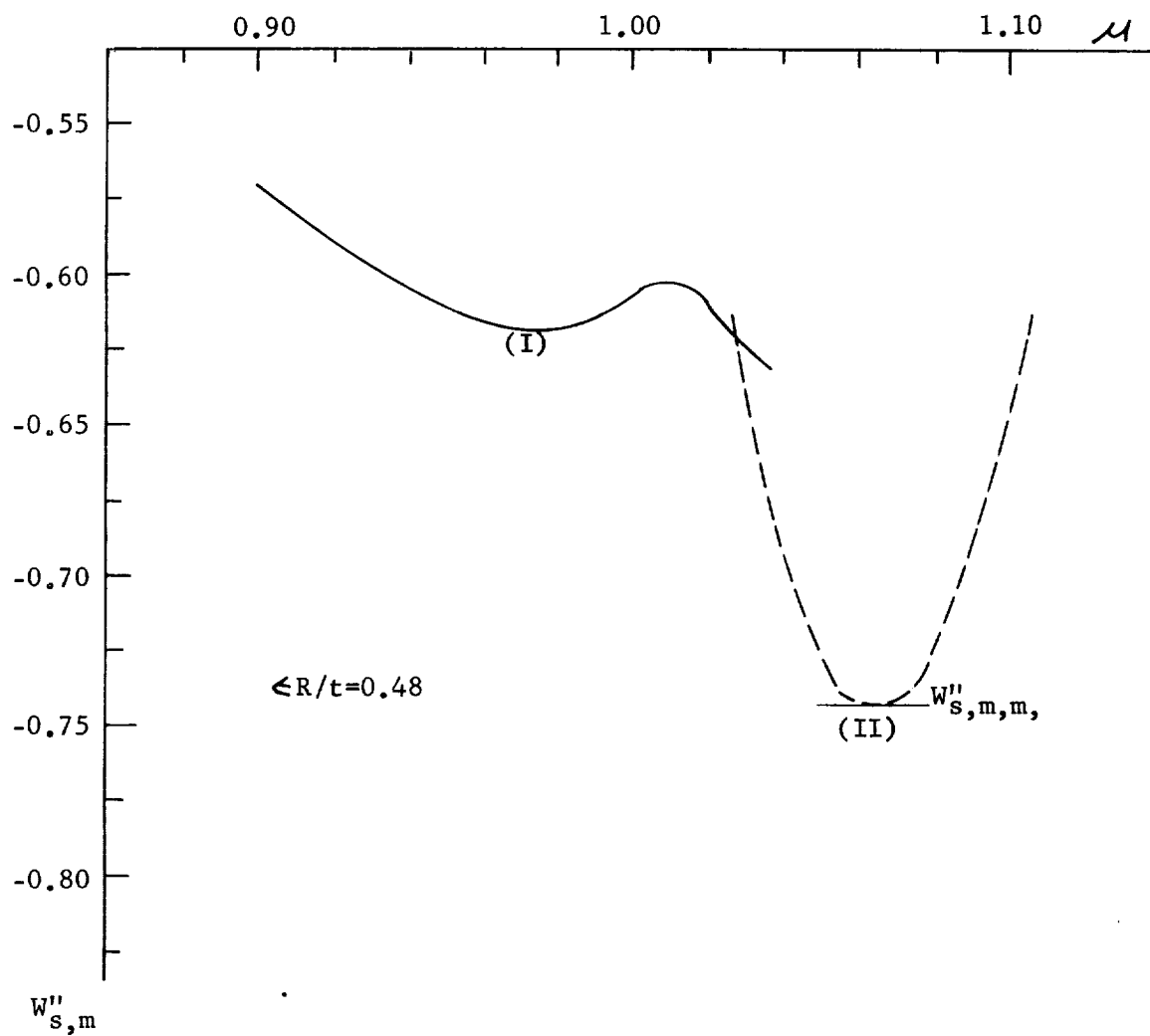


Fig.7 Variation of minimal values of W''_s with respect to μ against μ for the specific value $(\epsilon R/t) = 0.48$

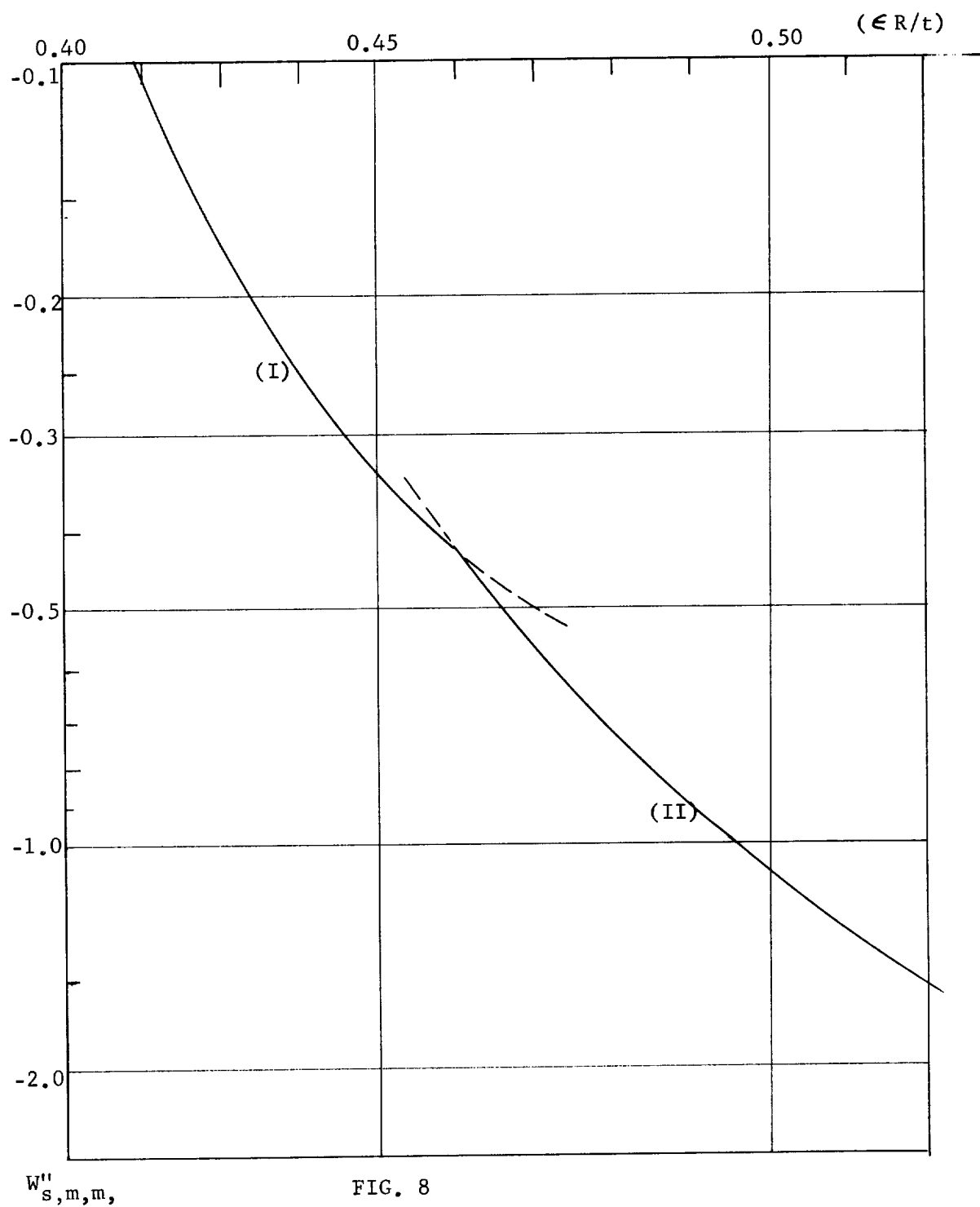


FIG. 8
Variation of the least minimal values of W''_s against $(\epsilon R/t)$

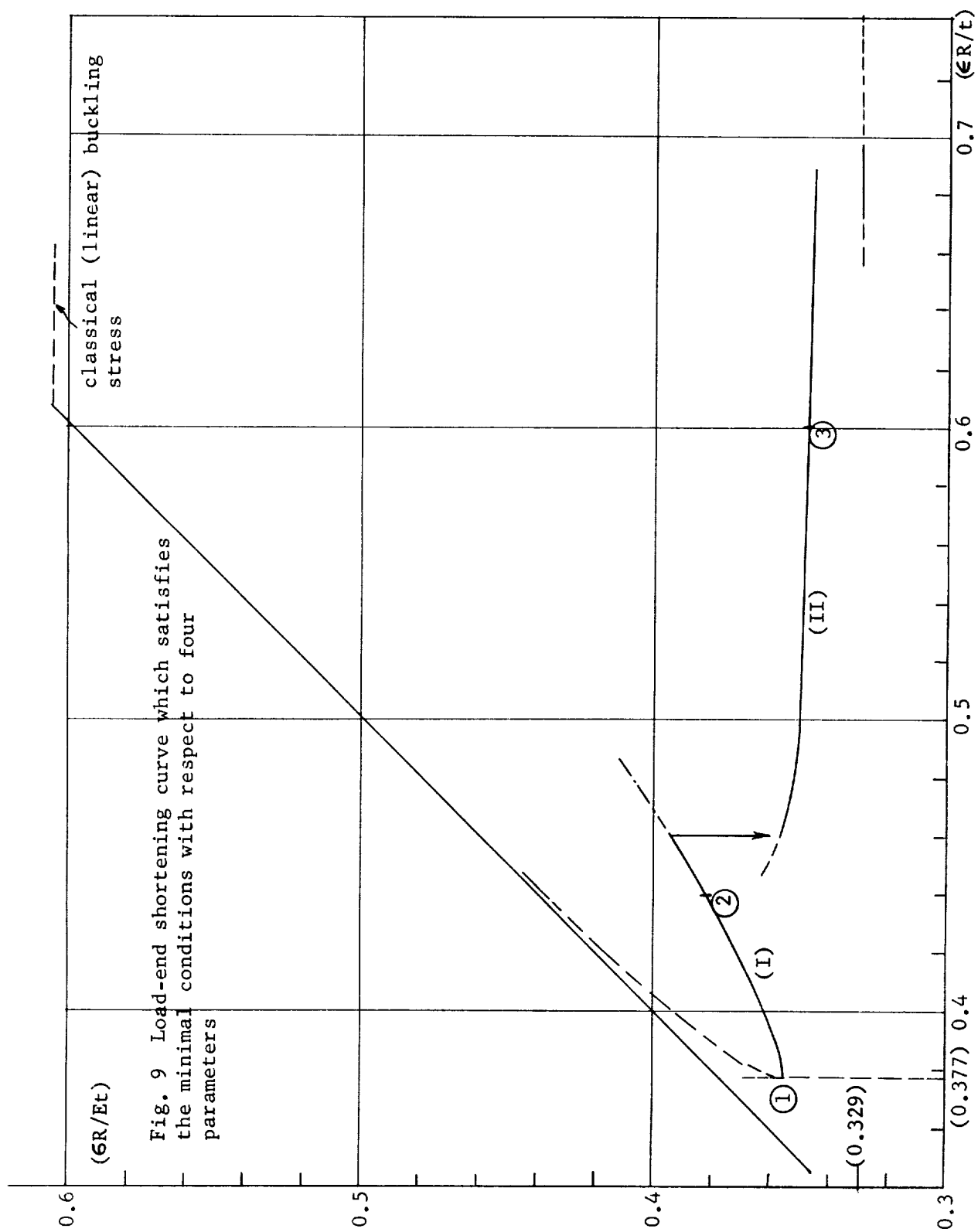


Fig. 9 Load-end shortening curve which satisfies the minimal conditions with respect to four parameters

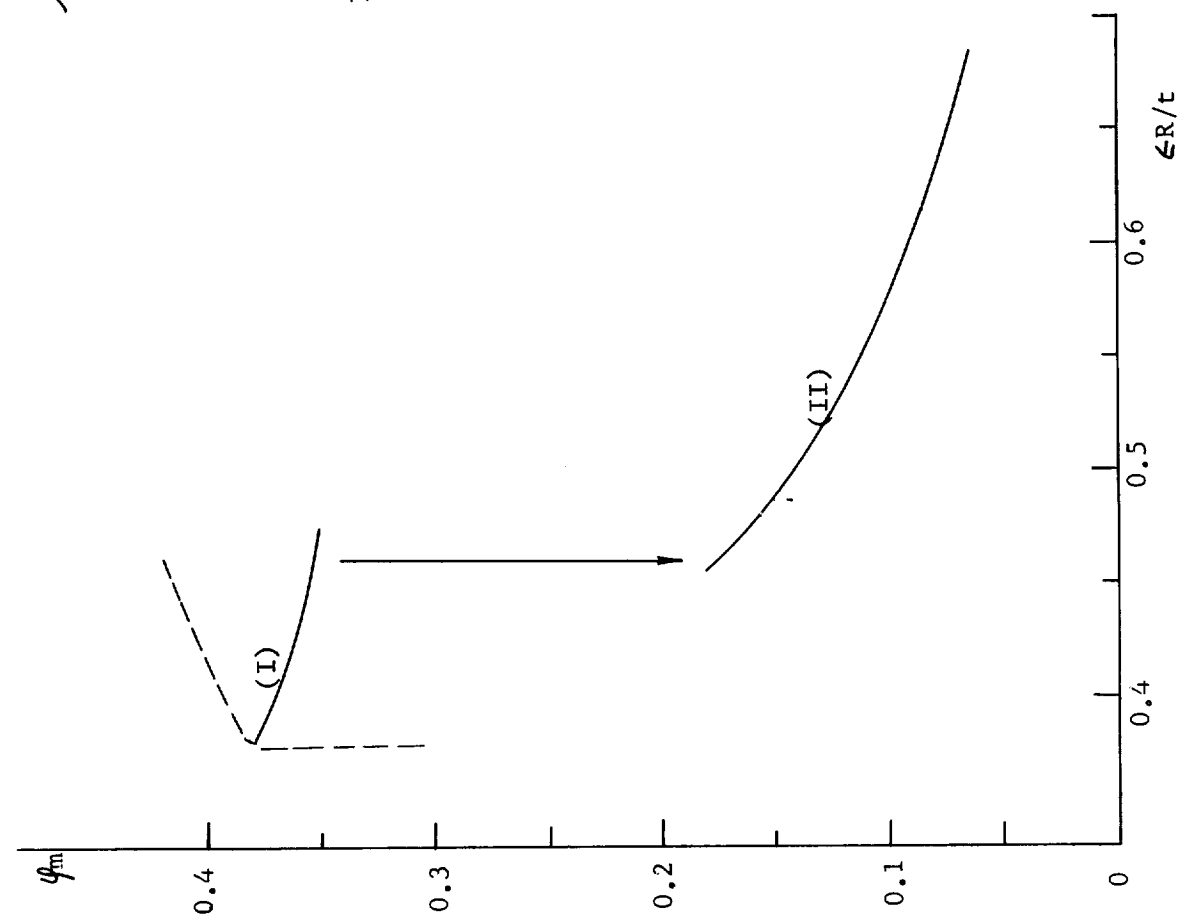


Fig.10 Variation of φ_m against $\epsilon R/t$

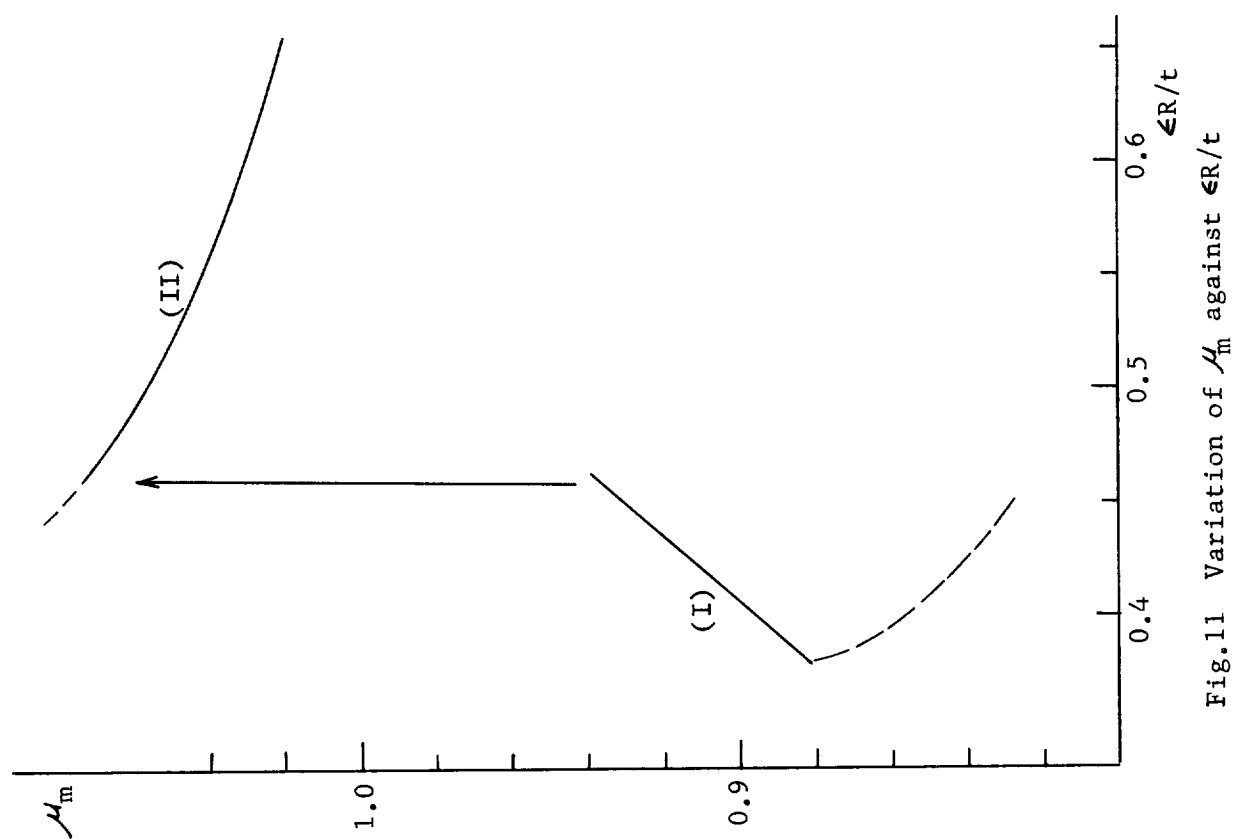


Fig.11 Variation of μ_m against $\epsilon R/t$

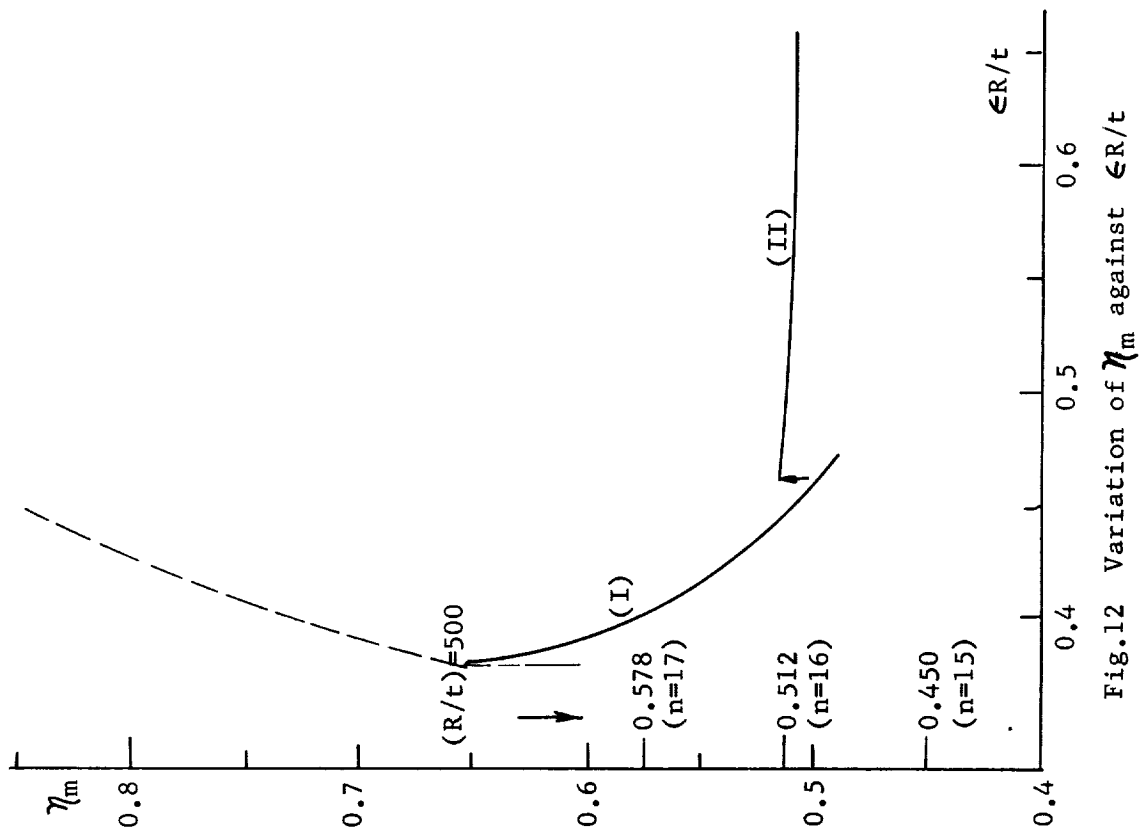


Fig.12 Variation of η_m against $\epsilon R/t$

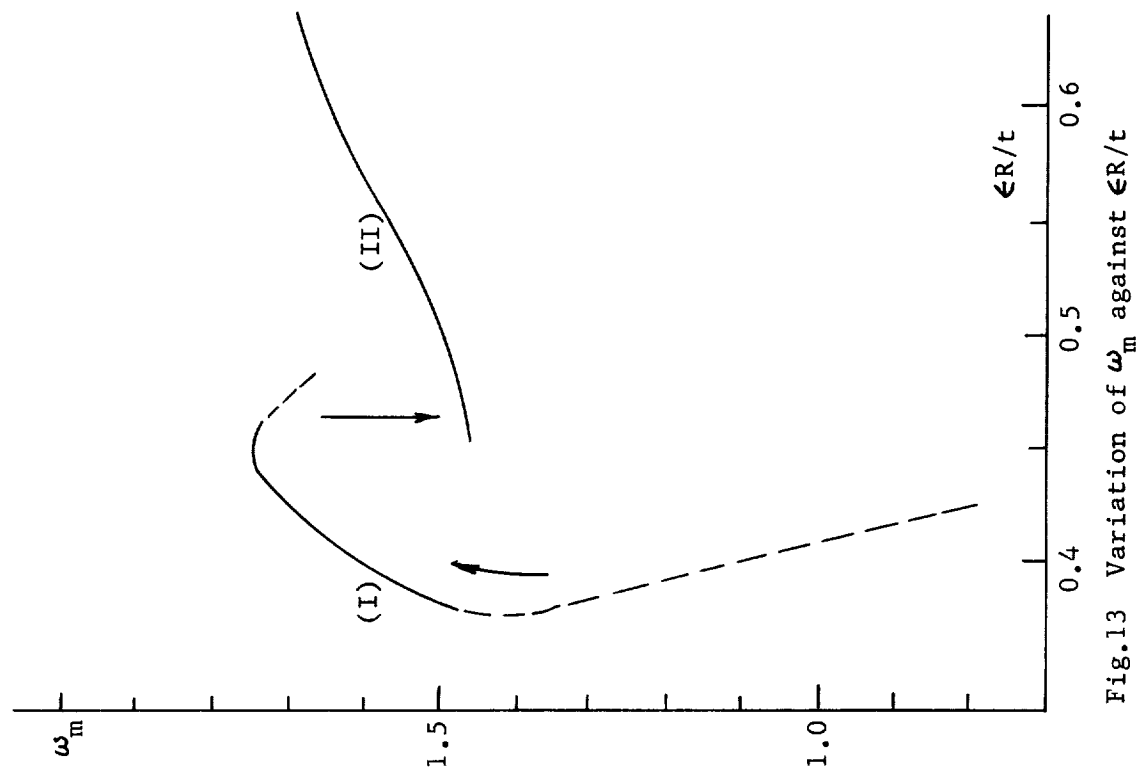


Fig.13 Variation of ω_m against $\epsilon R/t$

The variation of the deflection parameters g and h in the four parameters which are functions of μ and φ only in Eq.(42), is shown in Figs.14 and 15, respectively. As far as the other parameters of e and f are concerned, e is so small that it may be neglected, and f has a nearly constant value of about 1.52.

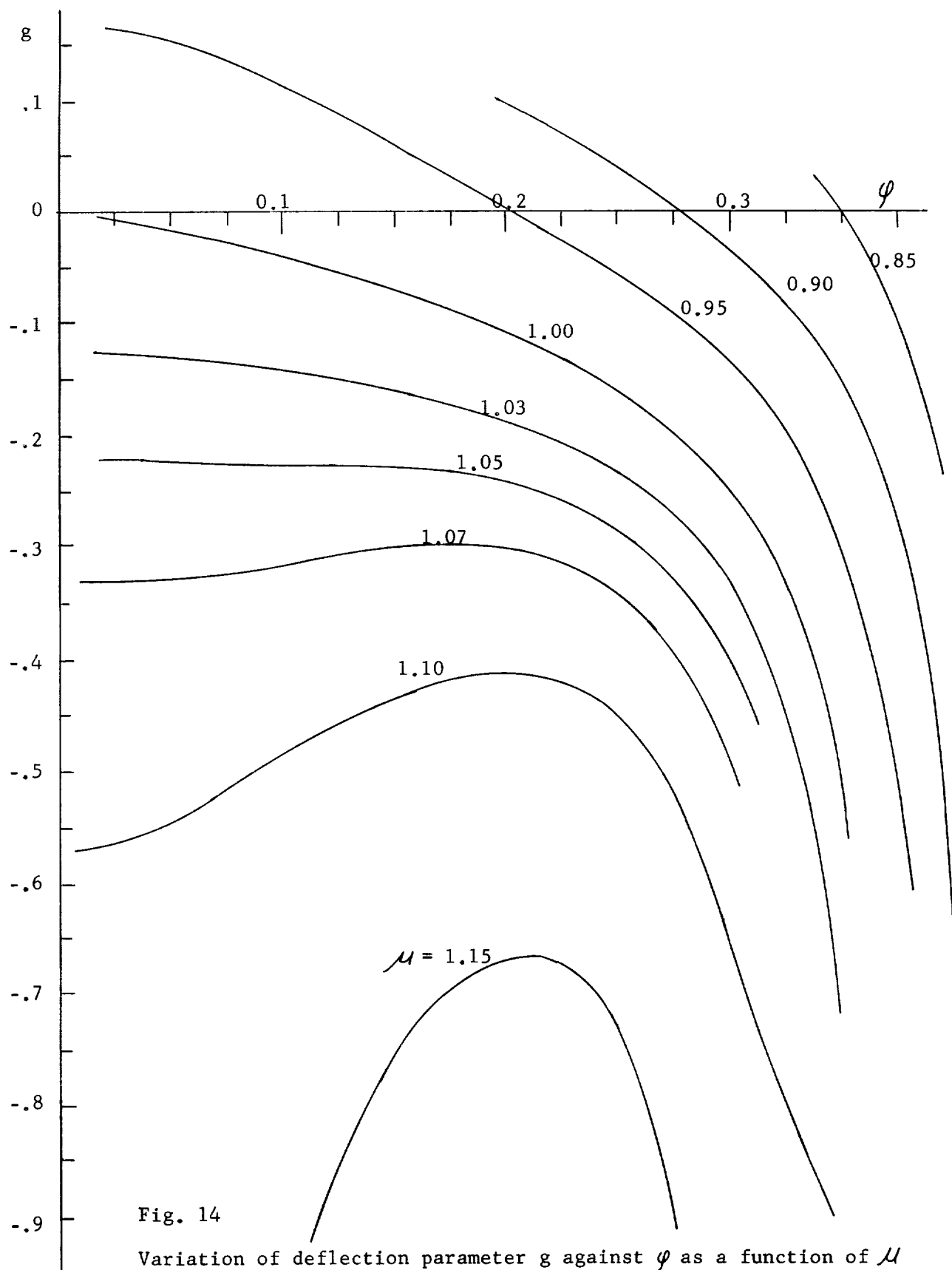


Fig. 14

Variation of deflection parameter g against φ as a function of μ

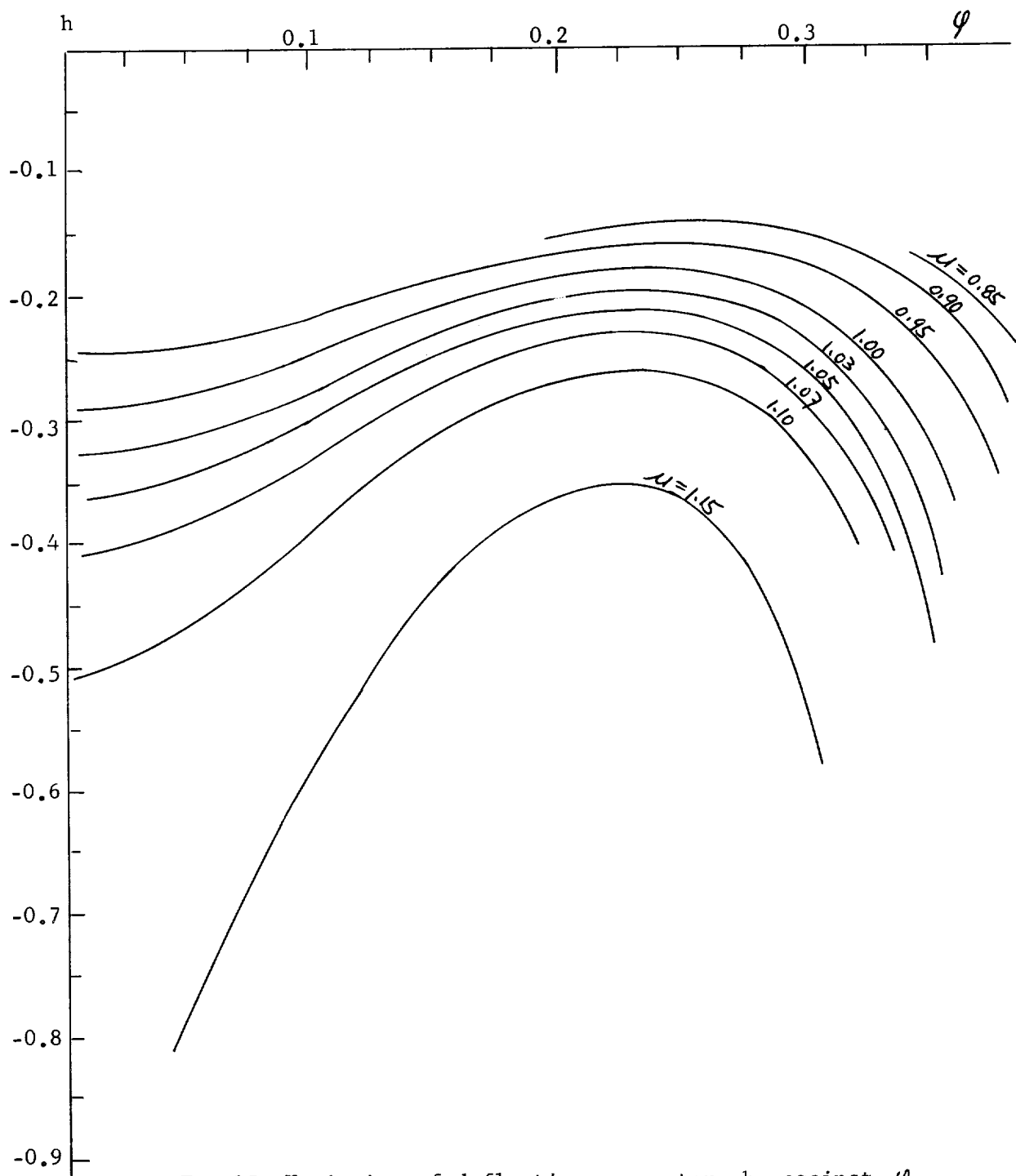


Fig.15 Variation of deflection parameter h against φ
as a function of μ

10. DISCUSSION

The numerical results obtained by the analysis will now be discussed as follows:

- (1) The minimal value of the axial stress in the possible equilibrium states after buckling was found to be about 0.329. This value is higher than those obtained by Kempner⁵ and Almroth⁶ for the case of overall buckling. It is believed that this result arises from the insufficient freedom of the assumed buckled pattern and from the incomplete satisfaction of the continuity conditions along the center lines. Taking into account more terms in the expression for the buckled pattern is expected to make it possible to satisfy more continuity-conditions, even though it will make the analysis much more complicated. In the case of larger values of φ , the violation of the continuity condition of the shearing stress, that is, of condition (B.8), seems to become rather serious. Accordingly, a refinement of the analysis is currently sought, by taking into account one more term with an arbitrary coefficient, so that this condition can be satisfied.
- (2) The total strain energy has a minimum with respect to the damping coefficient φ . The large values of φ give imaginary values of η which means that such cases cannot be realized. This suggests that the local buckling pattern is a favorable mode of deformation which is likely to arise in practice. This conclusion, which is confirmed by many experimental observations, represents the essential contribution of the present paper.
- (3) The ratio of the circumferential and axial wave lengths μ that gives the minimal values of W_s'' was found to be confined to a region close to 1.0, as seen in Fig. 11. The larger values of μ away from 1.0 give higher values of the strain energy, which means that only the nearly square diamond patterns can be realized, as is usually observed in experiments. In contrast, the values of μ obtained by Kempner⁵ vary within the wide range of 0.1 to 0.25 in the unstable region, and 0.25 to 1.2 in the stable region in the case of rigid-testing-machine loading; and the value of μ

corresponding to the minimal stress of 0.182 was found to be 0.362, even though the minimal value of the stress is closer to the experimental values.

(4) The effect of the length of the cylinder on the buckling stress has been fully analyzed before, even though it has been recognized in experimental work. This effect will be partly explained as follows.

The curvature parameter \sqrt{Rt}/L is one of the parameters in the expression for $\epsilon R/t$ of Eq.(63). Thus the load versus shortening curve depends on the value of \sqrt{Rt}/L , and some typical curves are shown in Fig.16 with three \sqrt{Rt}/L values. The curves shift to the right as \sqrt{Rt}/L increases, that is, as L becomes smaller. The smallest value of $(\epsilon R/t)$, $(\epsilon R/t)_{\min}$, serves as a lower bound for the occurrence of buckling in the case of rigid-testing-machine loading. The values of the stress $(R/Et)_{\min}$ corresponding to this minimal value of the shortening $(\epsilon R/t)_{\min}$ can be used as an estimate of the buckling stresses, even though it is necessary to jump over the rather high energy barrier with the aid of some external energy. The buckling stresses defined above are plotted in Fig.17 from which it can be seen that they become higher as the length of the cylinder decreases. The effect of the length of the cylinder is believed to be mainly due to the restriction along the boundaries, and it seems important to take into account the boundary conditions in the analysis of a shorter cylinder. However, the experimental evidence that the experimental buckling stress becomes higher for shorter cylinders, can be partly verified from such considerations of the effect of the curvature parameter \sqrt{Rt}/L .

(5) The buckled pattern obtained after satisfying the continuity conditions is rewritten as:

$$\frac{w}{t} = -v\left(\frac{\sigma R}{Et}\right) + \frac{1}{\eta}(2e^{-\beta x} - e^{-2\beta x})\left[\frac{1}{2}(e+fw^2) + \frac{1}{2}(g+hw^2)\cos 2ax + w \sin ax \sin by\right] \quad (42)$$

while the buckled pattern used by Kempner⁵ can be expressed as follows:

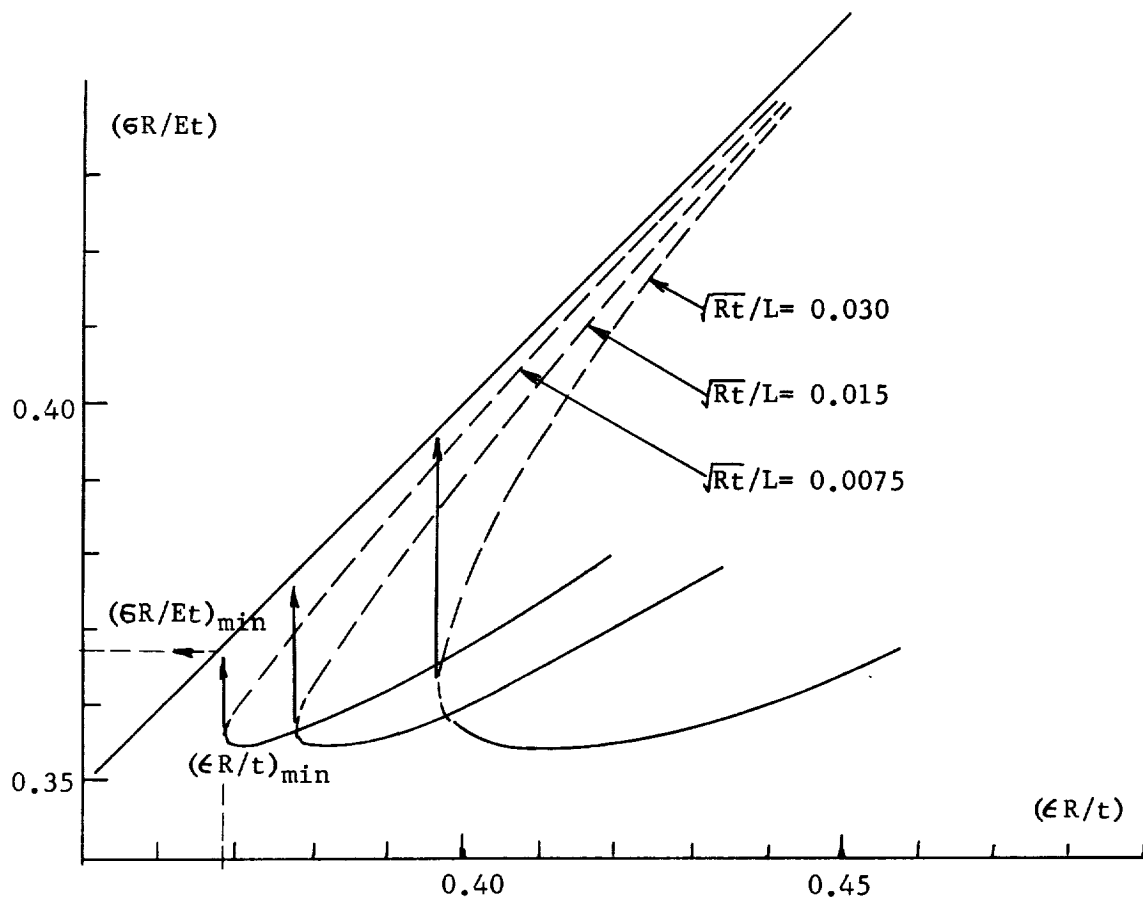


Fig.16 Change of axial load-end shortening curves as a function of curvature parameter \sqrt{Rt}/L

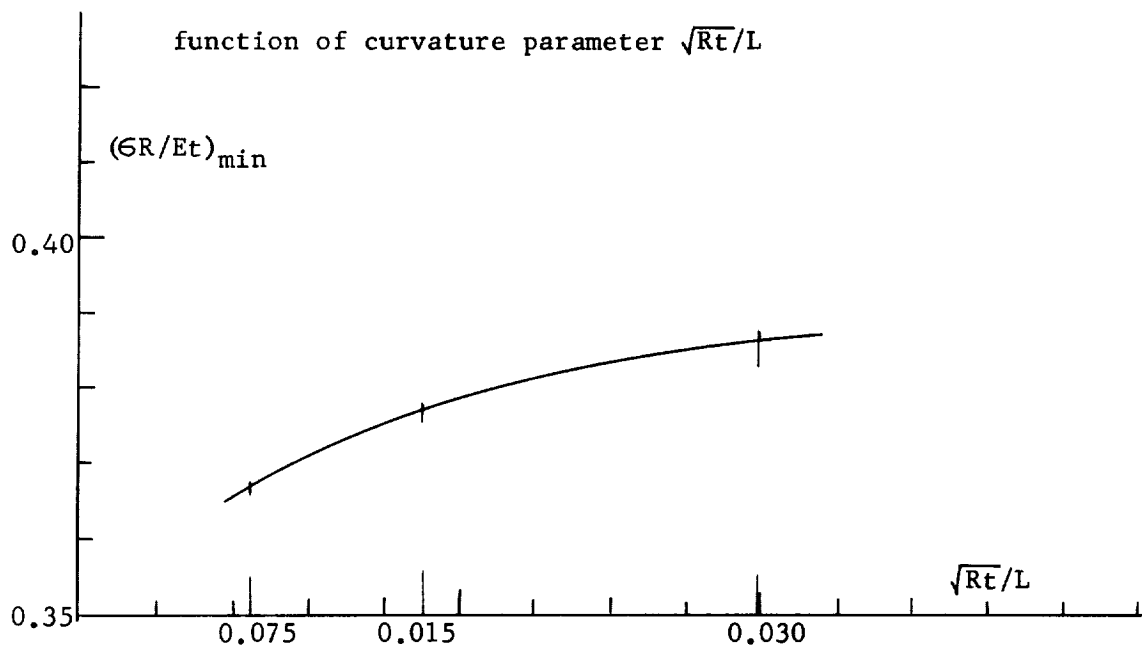


Fig.17 Variation of minimal possible buckling stress $(\sigma R/Et)_{\min}$ against curvature parameter \sqrt{Rt}/L

$$\frac{w}{t} = -v\left(\frac{\sigma R}{Et}\right) + \frac{1}{\eta} \left[\left(\frac{1}{8} + B^2 \right) \omega^2 - A\omega \cos 2ax + \omega \sin ax \sin by - B\omega \cos 2by \right] \quad (78)$$

by transferring the origin of coordinate to the middle point of a ridge as shown in Fig.2. The value of B was found to be very small, which will justify the neglect of the $\cos 2by$ term in this analysis. The first term in the bracket in which e is nearly zero and f is an approximately constant value around 0.152, corresponds to the first term of $1/8\omega^2$. The difference between the two patterns exists in the second term; that is to say, that in Eq.(42) is expressed in a parabolic form with respect to ω , while that in Eq.(78) is expressed in a linear form.

The wave patterns along $y = \lambda_y/\lambda^2$ are shown in Fig.18 for the three equilibrium points ① ② ③ referred to in Fig.9 as examples. The values of the deflection parameters for these points are listed in Table 1.

TABLE I

	①	②	③
$\left(\epsilon \frac{R}{t} \right)$	0.377	0.44	0.60
μ	0.88	0.923	1.029
ϕ	0.38	0.355	0.087
ω	1.40	1.745	1.65
η	0.65	0.515	0.508
e	0.0017	0.0011	0
f	0.1501	0.1509	0.1528
g	-0.250	-0.235	-0.137
h	-0.265	-0.235	-0.288
$\left(\frac{\sigma R}{Et} \right)$	0.355	0.3818	0.347

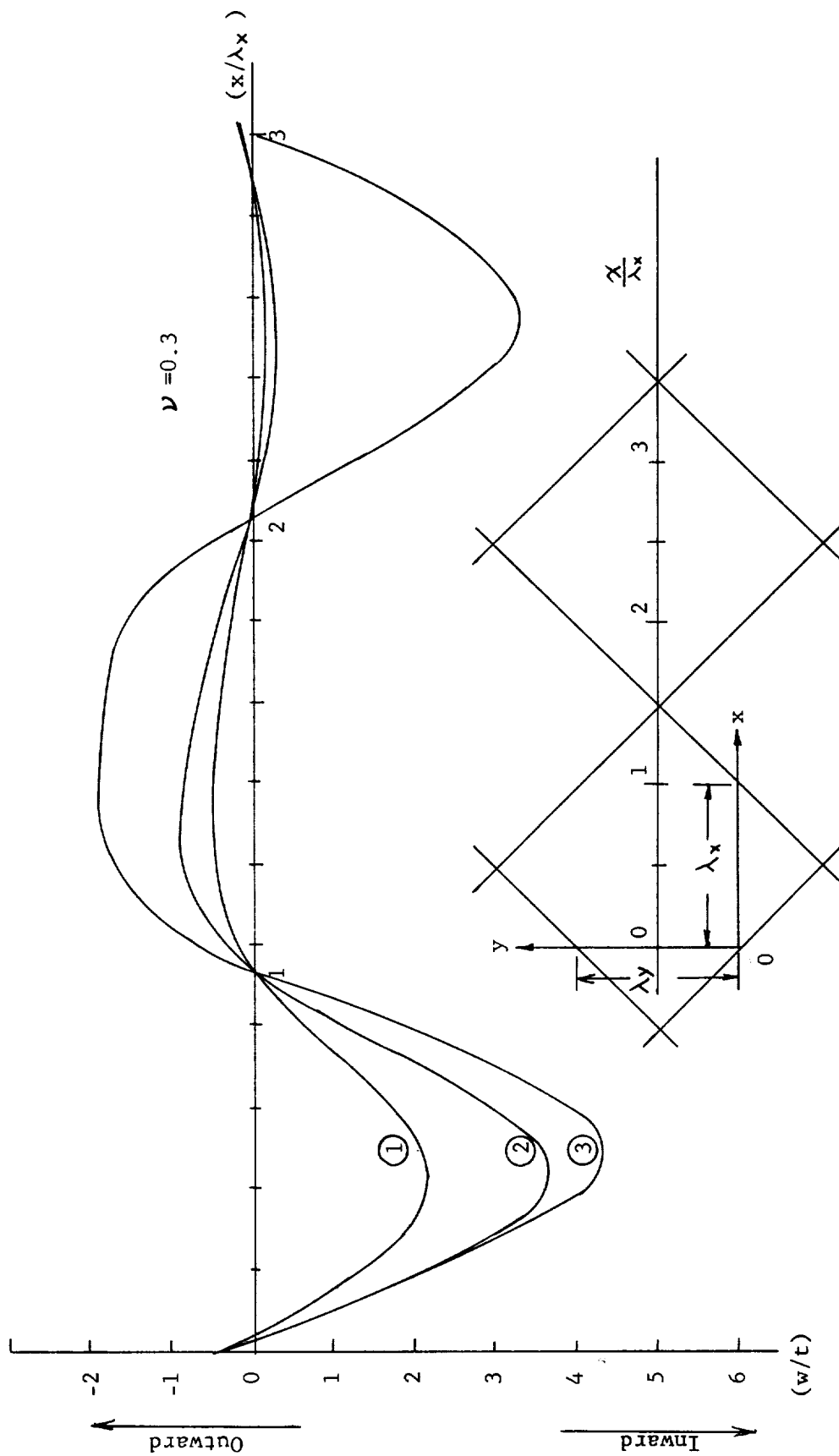


Fig.18 Wave patterns along the axial line $y = \lambda y / 2$ for three typical values of $(\epsilon R / t)$

The buckled patterns of ① and ② exhibit almost the two-tier type of buckle, but the damping in ③ is so small that this curve exhibits a nearly sinusoidal overall buckling pattern. However, it is expected that the damped pattern will be realized also in the range of larger shortening as will be explained below.

(6) Two stable equilibrium states were found to exist under a specified value of axial shortening. It will be reasonable to believe that the equilibrium state having the lowest value of the total strain energy is the most likely one after buckling. In this sense, the equilibrium curves marked (I) and (II) will be the most feasible stable states and the value of the $(\epsilon R/t)$ around 0.46 is the separating point of the two kinds of equilibrium states, of which (I) represents the highly damped pattern, while (II) represents the slowly damped pattern. It is unimportant that the two curves (I) and (II) are not connected continuously. The cylinder will not necessarily take the equilibrium position with the lowest level of energy in the postbuckling region, but the buckling will take place at a constant value of η , that is, with an integral number of circumferential waves. With increasing end shortening, the specimen will jump into a new and similar buckled pattern reducing the number of buckles by one, as seen in the experiments of Thielemann¹³. In order to snap from a stable equilibrium position of higher energy level to another stable equilibrium position, a finite amount of external energy must be supplied to the system. Accordingly, it can be imagined that the stable state (II) in the region of larger $\epsilon R/t$ will not be easily realized even though it has the lowest value of the energy.

The actual buckling is believed to follow the process shown in the schematic diagram of Fig.19 for the case of rigid-testing-machine loading. With increasing shortening beyond $(\epsilon R/t)_{\min}$, the shell will buckle easily into the region of state (I), which has a highly-damped buckling pattern, because the energy barrier corresponding to the unstable equilibrium state shown by the dotted line is very small. The equilibrium curve having a constant number of $n(\eta)$ will be followed for a while as the shell is continuously compressed. But at one point (say, for example, point (A)), the shell will snap through into another equilibrium curve ②

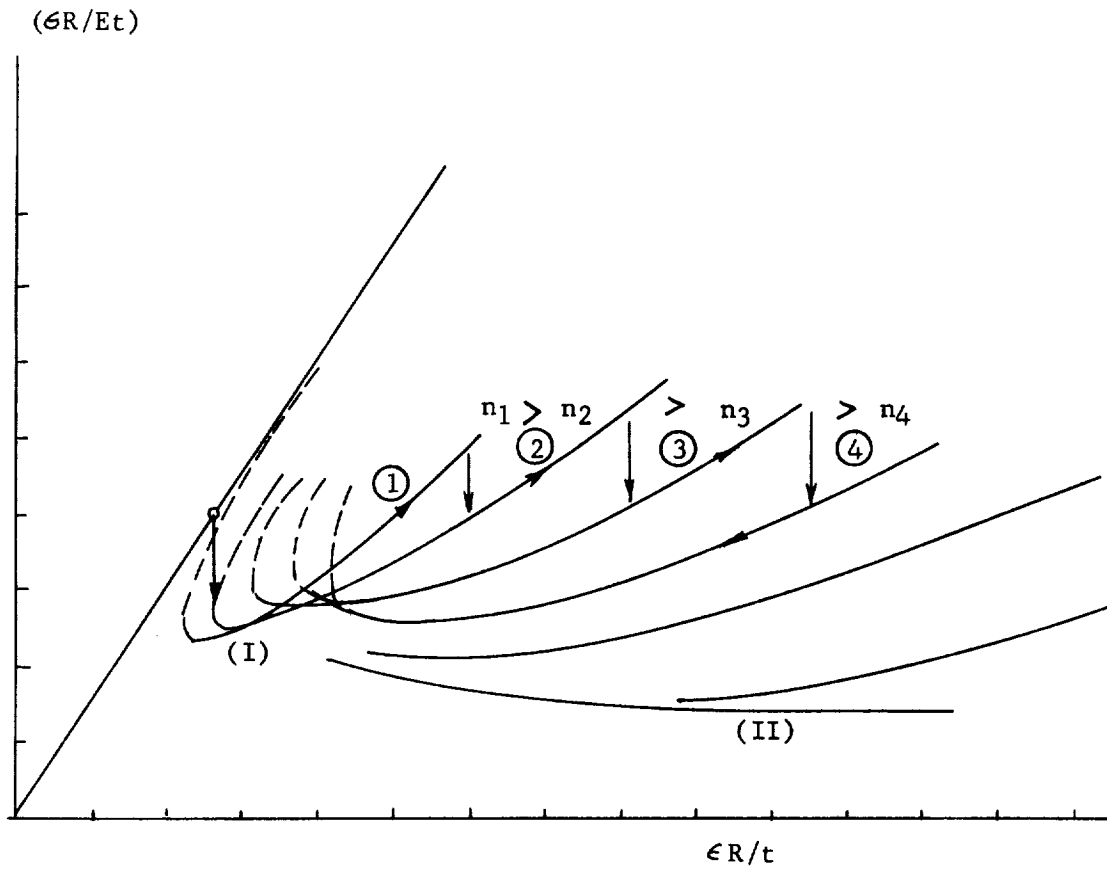


Fig.19 Schematic representation of buckling process for the case of rigid-testing-machine loading

having a value of n smaller by one, because the energy on ② is smaller than that on ①. As the shortening increases, the damping is expected to decrease as seen in Fig.10.

On the other hand, in the unloading process, the final curve marked ④ in Fig.19 will be followed for a while because the energy level is lower than that on the adjacent curves. The equilibrium curve belonging to category (II) which has smaller damping will not be realized unless the cylindrical shell is compressed considerably.

From the above considerations, it is thought that it is important to obtain the group of equilibrium curves for constant values of $n(\eta)$ in the investigation of the postbuckling behavior of shells. Such a treatment will be discussed in a forthcoming paper.

(7) In this paper, the effects of initial imperfections on the buckling stresses were not studied. Moreover, stability considerations were not given. The criterion of stability depends on the second variation of W'' or W' for the cases of rigid-testing-machine loading or dead-weight loading. It can be shown that the solid (lower) curve to the right of the minimal value of $\epsilon R/t$ has a positive value of the second variation of strain energy indicating a stable equilibrium state, while the dotted (upper) curve represents unstable equilibrium states. Although the first variations are the same for the two cases $\sigma = \text{constant}$ and $\epsilon = \text{constant}$, such will not be the case for the second variation. Both curves (I) and (II) are stable in the case of $\epsilon = \text{constant}$, but curve (II) will be an unstable and curve (I) will be only a locally stable state having a higher level of energy in the case of $\sigma = \text{constant}$. There is another stable state in the range of large deflections which was not considered here, because the buckling pattern without damping gives the lowest level of the total potential energy, and this analysis loses its accuracy in this region

REFERENCES

1. von Karman, Th., and Tsien, H. S., The Buckling of Thin Cylindrical Shells under Axial Compression, Jour.Aero. Sci., Vol.8, No.8, p.303, 1941/6.
2. Leggett, D. M. A., and Jones, R. P. N., The Behavior of a Cylindrical Shell under Axial Compression when the Buckling Load has been Exceeded, Rand M.2190; British Aeronautical Research Committee, 1942/8
3. Michielsen, H. F., The Behavior of Thin Cylindrical Shells after Buckling under Axial Compression, Jour. Aero. Sci., Vol.15, p.738, 1948/12.
4. Yoshimura, Y., On the Mechanism of Buckling of a Circular Cylindrical Shell under Axial Compression, Rept. of Inst. of Sci. & Tech., Tokyo Univ., Vol.5, No.5, 1951/11, (179/198); NACA TM.1390, 1955/7.
5. Kempner, J., Postbuckling Behavior of Axially Compressed Circular Cylindrical Shells, Jour. Aero. Sci., Vol.17, No.1, p.329/335, 342, 1954/5.
6. Almroth, B. O., On the Buckling of Circular Cylinders Subjected to Axial Compression, Report 6-90-61-115, 1962/7, Lockheed Missiles and Space Company.
7. Thielemann, W. F., New Developments in the Nonlinear Theories of the Buckling of Thin Cylindrical Shells, Proc. of Durand Centennial Conference, Aeronautics & Astronautics, edited by N. J. Hoff and W. G. Vincenti, Pergamon Press, 76/119.
8. Kanemitsu, S., and Nojima, N. M., Axial Compression Tests of Thin Circular Cylinders, M.S. Thesis, Calif. Inst. of Tech., 1939.
9. Tsien, H. S., A Theory for the Buckling of Thin Shells, Jour. Aero. Sci., Vol.9, No.10, p.373, 1942/8.
10. Hoff, N. J., Buckling of Thin Shells, AFOSR-TN-61-1422, SUDAER No.114, Department of Aero. and Astro., Stanford Univ., 1961/8; also, Proc. of the Th. von Kármán 80th Anniversary Symposium, Inst. of the Aerospace Sci., p.1, 1962.
11. Donnell, L. H., and Wan, C. C., Effect of Imperfections on Buckling of Thin Cylinders and Columns under Axial Compression, Jour. Appl. Mech., Vol.17, No.1, 1950/3, p.73.
12. Batdorf, S. B., Schildcrout, M., and Stein, M., Critical Stress of Thin-Walled Cylinders in Axial Compression, NACA Rept.No.887, Thirty-Third Annual Report, 1947, p.543.
13. Thielemann, W. F., On the Postbuckling Behavior of Thin Cylindrical Shells, Collected Papers on Instability of Shell Structures, NASA TN. D-1510, 1962/10, 203.

